

DATE ISSUED JUL 12 1990

**ornl**

ORNL/TM-11480

ORNL  
MASTER COPY

OAK RIDGE  
NATIONAL  
LABORATORY

MARTIN MARIETTA

The Superfluid Diffusion Equation

$$S(T) \frac{\partial T}{\partial t} = \nabla \cdot [K(T)(\nabla T)^{1/3}]$$

Lawrence Dresner

OPERATED BY  
MARTIN MARIETTA ENERGY SYSTEMS, INC.  
FOR THE UNITED STATES  
DEPARTMENT OF ENERGY

This report has been reproduced directly from the best available copy.

Available to DOE and DOE contractors from the Office of Scientific and Technical Information, P.O. Box 62, Oak Ridge, TN 37831; prices available from (615) 576-8401. FTS 625-8401.

Available to the public from the National Technical Information Service, 1215  
Department of Commerce, 5285 Port Royal Rd., Springfield, VA 22161.  
NTIS price codes—Final Copy: ACS Microfilm AD.

This report was prepared as an account of work sponsored by an agency of the United States Government. Neither the United States Government nor any agency thereof, nor any of their employees, makes any warranty, express or implied, or assumes any legal liability or responsibility for the accuracy, completeness, or usefulness of any information, apparatus, product, or process disclosed, or represents that its use would not infringe privately owned rights. Reference herein to any specific commercial product, process, or service by trade name, trademark, manufacturer, or otherwise, does not necessarily constitute or imply its endorsement, recommendation, or favor by the United States Government or any agency thereof. The views and opinions of authors expressed herein do not necessarily state or reflect those of the United States Government or any agency thereof.

Fusion Energy Division

## THE SUPERFLUID DIFFUSION EQUATION

$$S(T)\frac{\partial T}{\partial t} = \nabla \cdot [K(T)(\nabla T)^{1/3}]$$

Lawrence Dresner

Date Published: June 1990

Prepared for the  
Office of Fusion Energy  
Budget Activity No. 48 0B 00 90 4

Prepared by  
OAK RIDGE NATIONAL LABORATORY  
Oak Ridge, Tennessee 37831-6285  
operated by  
MARTIN MARIETTA ENERGY SYSTEMS, INC.  
for the  
U.S. DEPARTMENT OF ENERGY  
under contract DE-AC05-84OR21400

To Matthew, Danielle, Stephanie, and Micah

*"To see a world in a grain of sand."*

—*William Blake*



## CONTENTS

PREFACE . . . . .	vii
ACKNOWLEDGMENT . . . . .	ix
ABSTRACT . . . . .	xi
CHAPTER 1. SIMILARITY SOLUTIONS . . . . .	1
Introduction . . . . .	1
Similarity Solutions (Overview) . . . . .	2
The Ordinary Differential Equation for $y(x)$ . . . . .	6
Reduction of the Order of the Differential Equation . . . . .	9
Direction Field When $0 > \alpha > -2$ ( $\frac{4}{3} > \beta > 0$ ) . . . . .	13
Integration of the Differential Equation for $y(x)$ . . . . .	16
Further Discussion of the Similarity Solutions . . . . .	17
CHAPTER 2. APPLICATIONS OF SIMILARITY SOLUTIONS . . . . .	21
Introduction . . . . .	21
Stabilization of Superconductors . . . . .	23
Bubble Growth in Superheated He-II . . . . .	27
The Pulsed-Source Problem and the Pulsed Time-of-Flight Method of Measuring . . . . .	31
The Clamped-Flux Problem . . . . .	34
The Clamped-Temperature Problem when $K$ and $S$ Vary with Temperature . . . . .	39
CHAPTER 3. TIME-INDEPENDENT PROBLEMS; COMPLEMENTARY VARIATIONAL PRINCIPLES . . . . .	45
Introduction . . . . .	45
Comparison of the Superfluid and the Ordinary Conductance . . . . .	47
The Two-Dimensional, Irregularly Shaped Duct . . . . .	49
The Two-Dimensional, Irregularly Shaped Duct (continued) . . . . .	51
Tube Banks . . . . .	54
Constant Heat Source in an Irregular Volume . . . . .	58
CHAPTER 4. MAXIMUM AND MINIMUM PRINCIPLES . . . . .	59
Introduction . . . . .	59
The Maximum and Minimum Principles . . . . .	59
Constant Heat Source in a Square of Side 2 . . . . .	60
Pulsed-Source Problem in Spherical Geometry . . . . .	62
Proof of the Foregoing Assertions . . . . .	64

Discussion . . . . .	66
Pulsed-Source Problem in Cylindrical Geometry . . . . .	68
CONCLUDING REMARKS . . . . .	71
REFERENCES . . . . .	73

## PREFACE

This report deals with the superfluid diffusion equation

$$S(T)\frac{\partial T}{\partial t} = \nabla \cdot [K(T)(\nabla T)^{1/3}] \quad .$$

Although it is primarily about the mathematics of this equation, the results given here have a strongly practical aspect, because the superfluid diffusion equation describes heat transport in turbulent helium-II. (Helium-II, sometimes called superfluid helium, is a second liquid phase of helium that exists at temperatures below 2.17 K.) Recently, helium-II has been used to stabilize superconducting magnets, especially those for magnetic fusion or magnetic energy storage. It has also been proposed for cooling space-borne infrared telescopes. On account of such applications, it is helpful to have solutions to the superfluid diffusion equation such as those described here.

The superfluid diffusion equation is nonlinear owing to the appearance of the cube root of the temperature gradient. As a result, all the powerful methods of solution based on superposition are lost to us. But though much is lost, much remains. Three methods that do not depend on linearity—namely, the method of similarity, the variational method, and the method of maximum/minimum principles—form the mainstay of this report, and upon their foundation a substantial body of knowledge has been erected.

This work came about as the result of a four-year collaboration with the Applied Superconductivity Center of the University of Wisconsin—Madison during the period 1984–1988. The collaboration was principally with Professor S. W. van Sciver and the members of his group. Without Prof. van Sciver's unflagging interest in the results, his many suggestions for new work, and his constant encouragement, this report could never have reached its present satisfactory form.

Some of the results given in this report have been published before; other results are new. It is my feeling that all should be collected in one place, first, for the convenience of those who want to study the mathematical approach, and second, to make a tangible record of a very successful collaboration between Oak Ridge National Laboratory and the University of Wisconsin—Madison.

If these justifications for publishing this report are not enough, let me recall the somewhat lofty advice of the English mathematician G. H. Hardy that "it is one of the first duties of a professor . . . to exaggerate a little . . . the importance of his

subject.” And if this smacks too much of unhealthy hubris, let me take refuge in a humbler dictum of Faraday, who said simply: “Work, finish, publish.”

Lawrence Dresner  
Oak Ridge, Tennessee  
May 1989

## ACKNOWLEDGMENT

The manuscript on which this report is based could never have been turned into the elegant, eye-pleasing typescript that it has become without the skill and tireless devotion of Mrs. Sandra Vaughan. No words of thanks can ever express my gratitude to her. Truly, "her price is far above rubies."



## ABSTRACT

This report deals with the superfluid diffusion equation,  $S(T)\frac{\partial T}{\partial t} = \nabla \cdot [K(T)(\nabla T)^{1/3}]$ , which describes heat transport in turbulent helium-II (superfluid helium). Three methods of solution—the method of similarity, the variational method, and the method of maximum/minimum principles—are applied to this equation. The solutions discovered are helpful in addressing the use of helium-II in superconducting magnets and other applications.



## CHAPTER 1

### SIMILARITY SOLUTIONS

**Introduction.** The partial differential equation  $S(T)\frac{\partial T}{\partial t} = \nabla \cdot [K(T)(\nabla T)^{1/3}]$ , which is the central object of study of this report, describes heat transport in turbulent helium-II. The mechanism underlying this heat transport is very different from the diffusive mechanism of ordinary heat conduction, but thinking and speaking of heat transport in helium-II in the language of ordinary heat conduction is a useful heuristic and a convenient abbreviation. However, whereas ordinary heat conduction obeys Fourier's linear law  $\vec{q} = -k\nabla T$ , heat "conduction" in helium-II obeys the nonlinear law

$$\vec{q} = -K(\nabla T)^{1/3} . \quad (1.1)$$

Here  $\vec{q}$  is the heat flux vector [in watts per square meter ( $\text{W}\cdot\text{m}^{-2}$ )] and  $(\nabla T)^{1/3}$  is a vector whose magnitude is  $|\nabla T|^{1/3}$  and whose direction is that of  $\nabla T$ ;  $T$  is the temperature. The coefficient of proportionality  $K$  ( $\text{W}\cdot\text{m}^{-5/3}\cdot\text{K}^{-1/3}$ ) is a function of  $T$ , although it is often convenient to approximate it by some constant average value. We refer to  $K$  as the superfluid heat conductivity because superfluid helium is another name for helium-II.

If we apply the equation of continuity  $\nabla \cdot \vec{q} + ST_t = 0$  to Eq. (1.1), we obtain the superfluid diffusion equation

$$ST_t = \nabla \cdot [K(\nabla T)^{1/3}] . \quad (1.2)$$

The quantity  $S$  ( $\text{J}\cdot\text{m}^{-3}\cdot\text{K}^{-1}$ ), the heat capacity per unit volume, is also a function of  $T$ , but it, too, is often approximated by a constant average value. Equation (1.2) describes heat "conduction" in stagnant helium-II. From this point forward we drop the quotation marks, remembering that conduction in helium-II is qualitatively different from conduction in other materials.

The dependence of  $K$  and  $S$  on the temperature  $T$  is complicated, and it seems prudent to start by approximating  $K$  and  $S$  as constants. Then, to avoid the tedium of writing  $K$  and  $S$  over and over again, we can employ special units in which  $K = S = 1$ . A final answer obtained after calculation can be converted to a form correct in ordinary units by inserting, as needed, products of powers of  $K$  and  $S$  so as to make the final answer dimensionally homogeneous.

Now we turn our attention to the constant-property version of Eq. (1.2),

$$T_t = \nabla \cdot (\nabla T)^{1/3} . \quad (1.3)$$

In plane geometry, Eq. (1.3) can be written as

$$T_t = \left( T_z^{1/3} \right)_z, \quad (1.4)$$

which may be thought of as describing heat conduction in a thin, helium-II-filled pipe with insulated sides. Equation (1.4) is the jumping-off point for our investigations.

**Similarity Solutions (Overview).** The partial differential equation (1.4) is invariant to the one-parameter family of affine groups

$$\left. \begin{aligned} T' &= \lambda^\alpha T \\ t' &= \lambda^\beta t \\ z' &= \lambda z \end{aligned} \right\} 0 < \lambda < \infty, \quad (1.5)$$

where the constants  $\alpha$  and  $\beta$  are connected by a linear constraint,

$$M\alpha + N\beta = L. \quad (1.6)$$

The parameter  $\lambda$  labels the individual transformations of a single group. The parameter  $\alpha$  labels groups of the family. The coefficients  $M$ ,  $N$ , and  $L$  depend on the structure of the partial differential equation. In the case of Eq. (1.4),  $M = 2$ ,  $N = -3$ , and  $L = -4$ .

The truth of the assertions in the last paragraph is easily verified—if readers will assume that Eq. (1.4) holds for the unprimed variables and substitute Eq. (1.5) into Eq. (1.4), they will find that Eq. (1.4) also holds for the primed variables, but only if  $\alpha$  and  $\beta$  are connected by Eq. (1.6). The *use* of these assertions rests on the following considerations.

As we have just seen, if we have a solution  $T(z, t)$  of the partial differential equation, its image  $T'(z', t')$  under a transformation of the family (1.5) is also a solution. To clarify the meaning of this last statement, the following geometric interpretation is helpful. The solution  $T(z, t)$  represents a surface in the three-dimensional space in which  $T$ ,  $z$ , and  $t$  are the coordinates. Each point  $(T, z, t)$  on this surface is carried into another point  $(T', z', t')$  called its image under the transformation (which is labeled by a particular choice of  $\lambda$  and  $\alpha$ ). The locus of all the image points is another surface in  $(T, z, t)$  space, and it, too, represents a solution of the partial differential equation [since  $T'$ ,  $z'$ , and  $t'$  also obey Eq. (1.4)].

When  $\lambda$  varies over all possible values between 0 and  $\infty$ , the images of a given integral surface comprise a space-filling, one-parameter family of integral surfaces, each labeled by one value of  $\lambda$  and each of which is an image of any other. Among

the integral surfaces there may be some special ones whose images are the same as the original for all the transformations (all  $\lambda$ ) of one group (one  $\alpha$ ). Such integral surfaces (solutions) are said to be invariant to a group of the family. For them, the one-parameter family of image surfaces is not space-filling but consists only of the original surface itself.

An algebraic form for  $T(z, t)$  that has the property of being invariant to the group labeled by  $\alpha$  is

$$T(z, t) = t^{\alpha/\beta} y \left( z/t^{1/\beta} \right) , \quad (1.7)$$

where  $y$  is an as yet undetermined function of the simple argument  $x = z/t^{1/\beta}$ . [Proof:  $T' = \lambda^\alpha T = \lambda^\alpha \cdot t^{\alpha/\beta} y(z/t^{1/\beta}) = (t')^{\alpha/\beta} y(z'/(t')^{1/\beta})$ .] It can be shown,<sup>1</sup> though I shall not do it here, that Eq. (1.7) is the most general form an invariant solution can have.

Invariant solutions of the form (1.7) are interesting because when they are substituted into the partial differential equation, they lead to an *ordinary* differential equation for the as yet undetermined function  $y(x)$ . The reduction of the partial differential equation to an ordinary differential equation occurs, of course, because  $y$  is a function of a single argument only, namely,  $x = z/t^{1/\beta}$ .

It is shown in ref. 1 that the ordinary differential equation for  $y(x)$  is also invariant to a group of transformations, namely,

$$\left. \begin{array}{l} y' = \mu^{L/M} y \\ x' = \mu x \end{array} \right\} 0 < \mu < \infty , \quad (1.8)$$

where  $L$  and  $M$  are two of the coefficients in the linear constraint (1.6). The geometric interpretation of this invariance is the same as before: any integral curve  $y(x)$  is carried into another integral curve  $y'(x')$  by each transformation of the group (1.8), so that each integral curve belongs to a one-parameter family, all the members of which are images of one another.

The invariance of the ordinary differential equation for  $y(x)$  to the group (1.8) allows us to draw some valuable conclusions about the class of problems described by the boundary and initial conditions

$$\begin{aligned} T(z, 0) &= 0 , \\ T(\infty, t) &= 0 , \\ T(0, t) &= At^{\alpha/\beta} . \end{aligned} \quad (1.9)$$

In this class of problems, it is useful to think of  $T$  as the temperature *rise*, which is allowable for the constant-property equation (1.4). The problems then describe the temperature distribution in a semi-infinite pipe, initially at a constant temperature, in which the temperature rise at the front face varies as a power of the time.

The three boundary and initial conditions (1.9) for  $T$  collapse to the two boundary conditions

$$y(0) = A , \quad (1.10)$$

$$y(\infty) = 0$$

if  $\beta > 0$ . The image of  $y(x)$  under the group (1.8) obeys the same differential equation as  $y(x)$  and the boundary conditions

$$y'(0) = \mu^{L/M} A , \quad (1.11)$$

$$y'(\infty) = 0 .$$

Thus, if we know the solution  $T(z, t)$  for one value of  $A$ , we can find it for any other value of  $A$  by transforming  $y(x)$  with the group (1.8).

The heat flux through the front surface  $z = 0$  of the half-space can be calculated from the derivative

$$T_z(0, t) = t^{(\alpha-1)/\beta} \dot{y}(0) . \quad (1.12)$$

It follows from Eq. (1.8) that  $\dot{y}' = \mu^{(L/M)-1} \dot{y}$ , so that

$$\frac{\dot{y}'(0)}{[y'(0)]^{1-M/L}} = \frac{\dot{y}(0)}{[y(0)]^{1-M/L}} . \quad (1.13)$$

Equation (1.13) means that the ratio displayed is independent of the particular solution being considered, that is, is independent of  $y(0) = A$ . Let us call this ratio  $C$ . Then

$$\begin{aligned} T_z(0, t) &= t^{(\alpha-1)/\beta} C [y(0)]^{1-M/L} \\ &= C t^{(\alpha-1)/\beta} \times t^{(M/L-1)(\alpha/\beta)} \left[ t^{\alpha/\beta} y(0) \right]^{1-M/L} \\ &= C t^{-N/L} [T(0, t)]^{1-M/L} . \end{aligned} \quad (1.14)$$

So for all the problems of the class described by the boundary and initial conditions (1.9), the temperature rise and its derivative at  $z = 0$  are connected by the relation (1.14).

To see the meaning of this relation, let us insert the values  $L = -4$ ,  $M = 2$ , and  $N = -3$  appropriate to the superfluid diffusion equation. Then

$$-[T_z(0, t)]^{1/3} = -C^{1/3}t^{-1/4} [T(0, t)]^{1/2} . \quad (1.15)$$

Now, for example, when  $\alpha = 0$ , the temperature rise  $T(0, t)$  at the front face of the half-space is clamped at the constant value  $A$ . Then Eq. (1.15) says that the heat flux through the front surface varies inversely as the one-fourth power of the elapsed time and directly as the square root of the clamped-temperature rise. When  $\alpha = 1$ , the heat flux  $-[T_z(0, t)]^{1/3}$  at the front face is clamped at the constant value  $\dot{y}(0)$ . Then Eq. (1.15) says that the temperature rise at the front surface varies directly as the square root of the elapsed time and the square of the clamped heat flux. When  $\alpha$  has other values, neither the temperature rise nor the heat flux at the front face is clamped at a constant value, but though both vary in time, they are constrained to obey Eq. (1.15). The constant  $C$  in general depends on  $\alpha$  but not on  $y(0)$  or  $\dot{y}(0)$ .

Up to this point, we have not used any properties of the partial differential equation save its invariance to the family of groups (1.5). The conclusions that we have drawn so far are thus solely consequences of that invariance. Later, we shall derive them again by direct computation when we calculate the solutions  $y(x)$  in detail. But these computations, based on the specific properties of the partial differential equation, obscure the more general, group-theoretic nature of the foregoing equations, especially Eqs. (1.8), (1.13), and (1.14). It is to emphasize this group-theoretic origin that I have written this rather lengthy overview.

The form (1.7) is invariant to one group of the family (1.5), namely, the one corresponding to the specified values of  $\alpha$  and  $\beta$ . The form

$$T(z, t) = Uz^{L/M}t^{-N/M} , \quad (1.16)$$

where  $U$  is a constant, on the other hand, is invariant to all the groups of the family, no matter what the values of  $\alpha$  and  $\beta$  [as long as they satisfy the constraint (1.6)]. It can be shown, though I shall not do so here, that Eq. (1.16) is the most general form having this property. The constant  $U$ , like the function  $C(\alpha)$ , cannot be determined by group-theoretic arguments. The simplest way to determine it is to substitute the form (1.16) into the partial differential equation. If we do this for Eq. (1.4), for example, we find  $U = 4/3\sqrt{3}$ .

The most important of these group-theoretic results is the existence of the group (1.8), to which the ordinary differential equation for  $y(x)$  is invariant. In the case of

the superfluid diffusion equation, and in many other practical problems as well, this ordinary differential equation is of second order. Its invariance to the group (1.8) can be used to reduce it to a first-order differential equation according to a theorem of Lie. Lie's theorem says that if we choose as new variables a group invariant  $u(x, y)$  and a first differential invariant  $v(x, y, \dot{y})$ , the second-order differential equation for  $y$  in terms of  $x$  will reduce to a first-order differential equation for  $v$  in terms of  $u$ . A group invariant  $u(x, y)$  is a function of  $x$  and  $y$  such that  $u(x', y') = u(x, y)$ ; a first differential invariant  $v(x, y, \dot{y})$  is a function of  $x$ ,  $y$ , and  $\dot{y}$  such that  $v(x', y', \dot{y}') = v(x, y, \dot{y})$ . For the simple group (1.8), a suitable choice of  $u$  and  $v$  is

$$u = y/x^{L/M} , \quad (1.17a)$$

$$v = \dot{y}/x^{L/M-1} . \quad (1.17b)$$

An equally valid choice is

$$u = f\left(y/x^{L/M}\right) , \quad (1.17c)$$

$$v = g\left(y/x^{L/M}, \dot{y}/x^{L/M-1}\right) . \quad (1.17d)$$

The reduction of a second-order differential equation to first order helps us greatly because the content of a first-order equation can be visualized by means of its direction field. The existence of the group (1.8) and its use in reducing the second-order differential equation for  $y(x)$  to a first-order differential equation for  $v(u)$  are the subject of the author's earlier book,<sup>1</sup> which gives proofs of the unsupported statements made here. Readers interested in the group-theoretic background of the calculations that follow may wish to consult ref. 1, but they need not do so as long as they have the framework described above firmly in mind.

**The Ordinary Differential Equation for  $y(x)$ .** The partial derivatives of the invariant solution (1.7) can be calculated using the chain rule for differentiation:

$$\begin{aligned} T_t &= t^{\alpha/\beta-1} (\alpha y - x \dot{y}) / \beta , \\ T_z &= t^{(\alpha-1)/\beta} \dot{y} , \\ \left(T_z^{1/3}\right)_z &= t^{(\alpha-4)/3\beta} \frac{d}{dx} \left(\dot{y}^{1/3}\right) . \end{aligned} \quad (1.18)$$

Now according to Eq. (1.4), the first and third lines display equal quantities. Because of the constraint (1.6),  $(\alpha - 4)/3\beta = \alpha/\beta - 1$  when  $M = 2$ ,  $N = -3$  and  $L = -4$ . Therefore, the quantities in the first and third lines each contain as a factor the same power of  $t$ . When it is cancelled, we find

$$\beta \frac{d}{dx} (\dot{y}^{1/3}) + x\dot{y} - \alpha y = 0 . \quad (1.19)$$

It can be verified at once that Eq. (1.19) is invariant to Eq. (1.8) with  $L/M = -2$ .

Equation (1.19) can be solved as it stands in two cases, namely,  $\alpha = 0$  and  $\alpha = -1$ , and both of these solutions are of great practical importance. When  $\alpha = 0$  (and  $\beta = \frac{4}{3}$ ) we can immediately integrate Eq. (1.19) once by considering  $\dot{y}^{1/3}$  to be a new dependent variable. The result is

$$\dot{y} = - \left( \frac{3}{4} x^2 + \frac{1}{a^2} \right)^{-3/2} , \quad (1.20)$$

where  $a$  is a constant of integration. A second integration gives

$$y = \frac{2a^2}{\sqrt{3}} \left[ 1 - \frac{x}{(x^2 + 4/3a^2)^{1/2}} \right] . \quad (1.21)$$

The constant arising in the second integration has been chosen to make  $y(\infty) = 0$ , as required by the second of the boundary conditions (1.10).

According to Eq. (1.21),  $y(0) = 2a^2/\sqrt{3}$  and  $\dot{y}(0) = -a^3$ . Thus  $C \equiv \dot{y}(0)/[y(0)]^{3/2} = -3^{3/4}/2\sqrt{2}$  and is independent of  $a$ , as expected. Direct computation then shows that

$$- [T_z(0, t)]^{1/3} = \frac{3^{1/4}}{\sqrt{2}} t^{-1/4} [T(0, t)]^{1/2} , \quad (1.22)$$

exactly as expected from Eq. (1.15).

When  $x \gg 1$ ,  $y \sim 4/3\sqrt{3}x^2$ , which is independent of  $a$ . Thus, all the curves of the family (1.21) have the same asymptotic form when  $x$  is large. Since  $x \equiv z/t^{3/4}$ ,

$$T \sim \frac{4}{3\sqrt{3}} \frac{t^{3/2}}{z^2} \quad (x \gg 1) , \quad (1.23)$$

which is exactly the same as the totally invariant solution (1.16). As we shall see later, this is no coincidence and could have been predicted even if we did not know the explicit formula (1.21).

Since  $\alpha = 0$  characterizes the clamped-temperature problem, we give below the form of the solution (1.21) when the constant  $a$  is removed in favor of the constant  $A \equiv y(0) = 2a^2/\sqrt{3}$ :

$$\frac{T}{A} = \frac{y}{A} = 1 - \frac{X}{\left( X^2 + \frac{8}{3\sqrt{3}} \right)^{1/2}} , \quad (1.24a)$$

$$X = x\sqrt{A} = z\sqrt{A}/t^{3/4} . \quad (1.24b)$$

To reconstitute this equation so that it applies in any set of units (rather than the special units in which  $K = S = 1$ ), we leave the first line unchanged and replace the second line by the dimensionally homogeneous equation

$$X = z \left( \frac{S}{Kt} \right)^{3/4} \sqrt{A} \quad (1.25)$$

(remember that  $A$  has the units of temperature).

The solution (1.24) has been made the basis of a theory of stabilization of superconductors by helium-II. This theory is discussed in Chap. 2, and we now pass on to discuss the second case in which Eq. (1.19) can be solved, namely,  $\alpha = -1$  ( $\beta = \frac{2}{3}$ ). In this case

$$T = t^{-3/2} y \left( \frac{z}{t^{3/2}} \right), \quad (1.26)$$

so that

$$\int_{-\infty}^{+\infty} T dz = \int_{-\infty}^{+\infty} y(x) dx \quad \left( x = z/t^{3/2} \right). \quad (1.27)$$

Since the integral on the right-hand side of Eq. (1.27) is a pure number, the integral on the left-hand side, though nominally a function of  $t$ , is actually constant. If we again interpret  $T$  as the temperature rise, then  $T dz$  is proportional to the heat required to raise the temperature in the interval  $dz$  of an infinite pipe by the amount  $T$ . The constancy of the integral on the left-hand side of Eq. (1.27) then implies the constancy in time of the total heat added to the helium-II in the pipe. If we can find a solution to Eq. (1.19) that is sharply peaked for small  $t$  and spreads out as  $t$  increases, we can use it to describe the dispersion of a heat pulse uniformly deposited (at  $t = 0$ ) in some plane cross section of the pipe (which we take to be  $z = 0$ ).

When  $\alpha = -1$ , Eq. (1.19) is a perfect differential and can be integrated to give

$$\frac{2}{3} \dot{y}^{1/3} + xy = 0. \quad (1.28)$$

The constant of integration on the right-hand side of Eq. (1.28) has been taken to be zero since  $\dot{y}(0) = 0$  on account of the symmetry of  $y(x)$ . A second integration now gives

$$y = \frac{4}{3\sqrt{3}} (x^4 + B^4)^{-1/2}, \quad (1.29)$$

where  $B$  is a second constant of integration. Since  $\dot{y}(0) = 0$ ,  $C = 0$  when  $\alpha = -1$ . When  $x \gg 1$ ,  $y$  is again asymptotic to  $4/3\sqrt{3}x^2$ , independent of  $B$ . When this asymptotic form is substituted into Eq. (1.26), we again find that the asymptotic form of  $T$  is given by Eq. (1.23); as noted previously, this is the same as the totally invariant solution (1.16).

The constant  $B$  is related to the value  $Q$  of the integral in Eq. (1.27):

$$QB = 2\Gamma^2 \left( \frac{1}{4} \right) / 3\sqrt{3}\pi = 2.854535\dots \quad (1.30)$$

When Eq. (1.29) is reconstituted so that it applies in any set of units, it takes the form

$$\frac{T}{(Q/S)^2} \left( \frac{Kt}{S} \right)^{3/2} = \frac{4}{3\sqrt{3}} (X^4 + b^4)^{-1/2}, \quad (1.31)$$

where

$$X = \frac{Qz}{S} \left( \frac{S}{Kt} \right)^{3/2} \quad (1.32)$$

and  $b$  is the numerical constant on the right-hand side of Eq. (1.30). Here  $Q$  is to be interpreted as the pulse energy per unit cross-sectional area and has the units  $\text{J}\cdot\text{m}^{-2}$  in the SI system.

The solution given in Eqs. (1.31) and (1.32) is sharply peaked for short times and spreads out as time goes on. Therefore, it is the sought-for description of the evolution of a sudden heat pulse deposited at the center of an infinite tube. This situation has been studied experimentally and the results are described in Chap. 4, but it is worth noting here that the agreement with Eqs. (1.31) and (1.32) is extremely good.

**Reduction of the Order of the Differential Equation.** Equation (1.19) is not easily solvable for values of  $\alpha$  other than 0 and  $-1$ , and for all other values we proceed by introducing the new variables  $u = xy^{1/2}$  and  $v = x\dot{y}^{1/3}$  suggested by Lie's theorem. Then,

$$x \frac{dv}{dx} = v + x^2 \frac{d}{dx} \left( \dot{y}^{1/3} \right) = v + \frac{\alpha}{\beta} u^2 - \frac{1}{\beta} v^3 \equiv G(u, v), \quad (1.33a)$$

$$x \frac{du}{dx} = u + \frac{1}{2} \frac{v^3}{u} \equiv F(u, v), \quad (1.33b)$$

so that

$$\frac{dv}{du} = \frac{G(u, v)}{F(u, v)} = \frac{2u\beta v + \alpha u^2 - v^3}{\beta(2u^2 + v^3)}. \quad (1.34)$$

To understand the nature of the solutions  $v(u)$  of Eq. (1.34) we study its direction field. We restrict our attention to the fourth quadrant since  $u = x^{1/2}y > 0$  and  $v = x^{1/3}\dot{y} < 0$  because  $y > 0$  and  $\dot{y} < 0$ .

Solutions (1.7) that spread out as time advances correspond to  $\beta > 0$ . This restriction requires  $\alpha > -2$ . As we shall see subsequently, the direction field has two different forms depending on whether  $\alpha > 0$  or  $0 > \alpha > -2$ . We start our investigations with the first case, namely,  $\alpha > 0$  ( $\beta > \frac{4}{3}$ ).

To sketch a direction field it is convenient first to divide it into regions in each of which the slope  $dv/du$  has one sign only. These regions are separated by curves on which  $dv/du$  is either 0 or  $\pm\infty$ . Figure 1.1 shows these curves, labeled  $C_0$  and  $C_\infty$ . Each is identified with short hatch marks showing the slope  $dv/du$ . The singular points of the differential equation, which play a central role in what follows, are the points of intersection of  $C_0$  and  $C_\infty$ . They turn out to be the origin  $O:(0,0)$  and the point  $P:(2/3^{3/4}, -2/\sqrt{3})$ . The sign of the slope in the four regions into which the curves  $C_0$  and  $C_\infty$  separate the direction field is shown by the encircled plus and minus signs drawn in these regions. A moment's thought will then show that

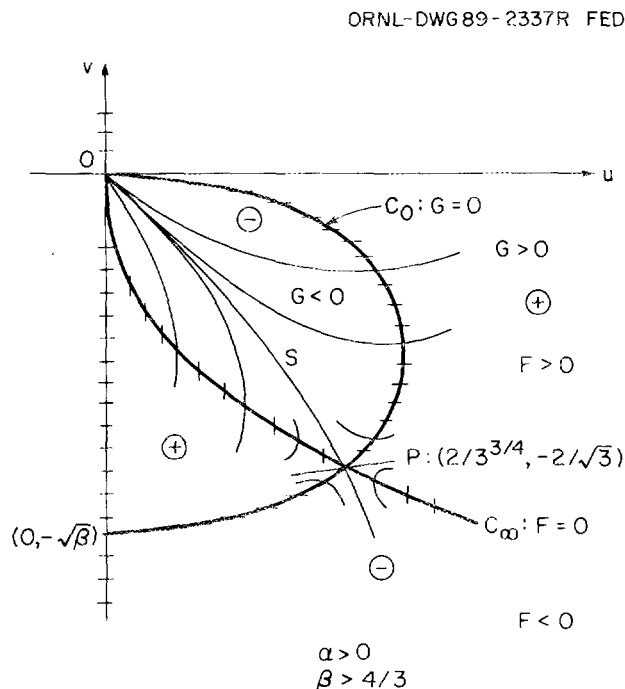


Fig. 1.1. The direction field of Eq. (1.34) with  $\alpha > 0$ .

the integral curves  $v(u)$  in the fourth quadrant must look as shown in the sketch (light lines) and that the point  $P$  is a saddle point.

As we have seen earlier, the integral curves  $y(x)$  obeying the boundary conditions (1.10) are all images of one another under the group (1.8). Now any curve  $y(x)$  defines a corresponding curve  $v(u)$  through the relations  $v = xy^{1/3}$  and  $u = xy^{1/2}$ . Two curves  $y(x)$  that are images of one another under (1.8) correspond to the *same* curve  $v(u)$  because  $v = xy^{1/3} = x'y^{1/3}$  and  $u = xy^{1/2} = x'y^{1/2}$ . So the entire family of solutions defined by the boundary conditions (1.10) all correspond to a single curve in the  $(u, v)$  plane.

The curve we are looking for must pass through the origin  $O$  because when  $x = 0$ ,  $u = v = 0$  if  $y(0)$  and  $\dot{y}(0)$  are finite. Among these curves, one stands out as different from all the rest, namely, the separatrix  $S$ . It is the one we want, and we prove this by showing that as the point  $(u, v)$  approaches  $P$  along  $S$  from the direction of  $O$ ,  $x$  approaches infinity.

If we approach the singular point  $P$  along an integral curve  $S$ :  $\frac{dv}{du} = m$ , then in the immediate vicinity of  $P$ , Eq. (1.33b) can be written

$$x \frac{du}{dx} = (F_u + mF_v)(u - u_P) \quad (1.35)$$

to lowest order. The partial derivatives  $F_u$  and  $F_v$  are to be evaluated at  $P$ . Equation (1.35) means that near  $P$

$$x = \text{const} \times (u - u_P)^{1/(F_u + mF_v)} . \quad (1.36)$$

Thus as  $u \rightarrow u_P$ ,  $x$  approaches 0 or  $\pm\infty$  according to whether  $F_u + mF_v$  is positive or negative. Now  $F_u + mF_v$  is the directional derivative of  $F$  along the curve  $S$  in the direction of increasing  $u$ . Since  $S$  and  $C_\infty : F = 0$  intersect at  $P$ ,  $F_u + mF_v$  is positive if  $S$  crosses  $C_\infty$  in the direction of increasing  $F$  and negative if  $S$  crosses  $C_\infty$  in the direction of decreasing  $F$ . These results are summarized below:

At a singular point  $P$ , if  $S$  crosses  $C_\infty : F = 0$  in *the direction of increasing  $u$* , and

$$\left. \begin{array}{l} \bullet F \text{ increases, } x \rightarrow 0 \\ \bullet F \text{ decreases, } x \rightarrow \pm\infty \end{array} \right\} \text{ as we approach } P \text{ along } S . \quad (1.37)$$

Exactly the same rule holds if we replace  $u$  by  $v$ ,  $C_\infty$  by  $C_0$ , and  $F$  by  $G$ . The limits 0 and  $\pm\infty$  are the only ones possible. The rule (1.37) enables us to tell at a glance what the limiting value of  $x$  is along any integral curve through a singularity.

In Fig. 1.1,  $F$  is positive above  $C_\infty$  and negative below  $C_\infty$ . By the rule (1.37), therefore,  $x \rightarrow \infty$  as  $u$  approaches  $P$  along  $S$  and  $x \rightarrow 0$  as  $u$  approaches  $O$  along  $S$  (we already knew this second fact). Now, when the point  $(u, v)$  is near  $P$ ,  $y = u_P^2/x^2 = 4/3\sqrt{3}x^2$ . This equation gives the asymptotic form of  $y$  for large  $x$  and shows that the family of solutions  $y(x)$  corresponding to the separatrix  $S$  obeys the second of the boundary conditions (1.10).

The constant in the asymptotic form is the same as the constant in the totally invariant solution (1.16). This is no accident, as we now demonstrate. The function  $y(x)$  belonging to the totally invariant solution is given by

$$t^{\alpha/\beta}y(x) = Uz^{L/M}t^{-N/M} . \quad (1.38)$$

Now, since  $N/M + \alpha/\beta = L/M\beta$ ,

$$y(x) = Uz^{L/M}t^{-L/M\beta} = Ux^{L/M} . \quad (1.39)$$

According to Eqs. (1.17c) and (1.17d), the curve in the  $(u, v)$  plane to which the solution (1.39) corresponds consists of only one point, namely, that for which

$$u = f(U) , \quad (1.40a)$$

$$v = g(U, LU/M) . \quad (1.40b)$$

For the solution (1.39)–(1.40),  $du/dx = 0$  and  $dv/dx = 0$  since  $u$  and  $v$  remain fixed as  $x$  and  $y$  change. Thus the point given by Eq. (1.40) is a singular point. Finally, along  $S$  near the singular point  $P$ ,  $y = f^{-1}(u_P)x^{L/M}$ . From Eq. (1.40a) we can see that  $f^{-1}(u_P) = U$ , the constant in the totally invariant solution (1.16). From the preceding we can also see that the totally invariant solution gives the asymptotic form for large  $z$  or small  $t$  of all the similarity solutions (1.7) no matter what the values of  $\alpha$  and  $\beta$ .

Now that we have seen how  $y(x)$  behaves for large  $x$  ( $u, v$  near  $P$ ) we may ask how  $y(x)$  behaves near  $x = 0$  ( $u, v$  near  $O$ ). To determine this, we must study the behavior of the integral curves  $v(u)$  near  $O$ , that is, when both  $u$  and  $v$  are  $\ll 1$ . In this limiting case,  $v = Eu$ ,  $E = \text{const}$ , satisfies Eq. (1.34) to lowest order. This latter phrase means neglecting higher powers of  $v$  against lower powers of  $v$  and

higher powers of  $u$  against lower powers of  $u$ . The constant  $E$  is not determined by Eq. (1.34) and can have any value. From  $v = Eu$  it follows at once that

$$E = \lim_{u \rightarrow 0} \left( \frac{v}{u} \right) = \lim_{x \rightarrow 0} \frac{xy^{1/3}}{xy^{1/2}} = \frac{\dot{y}^{1/3}(0)}{y^{1/2}(0)} = C^{1/3}, \quad (1.41)$$

where  $C$  is the ratio defined in Eq. (1.13).

To calculate  $E$ , we integrate Eq. (1.34) numerically from  $P$  to  $O$  along  $S$ . We choose this direction of integration because it is the direction in which the integral curves converge and the numerical integration is stable. Numerical integration in the opposite direction,  $O$  to  $P$ , is unstable. We cannot start the integration at the point  $P$  because  $P$  is a singular point. We overcome this difficulty by advancing a short distance along  $S$  to a new starting point. To make this advance, we need the slope of  $S$  at  $P$ , and this we calculate by applying L'Hospital's rule to Eq. (1.34). A short calculation shows that the two possible slopes at  $P$  have opposite signs when  $\alpha > 0$  and that the negative slope is given by

$$m = -\frac{\beta + 4 + [(\beta + 4)^2 + 16\alpha\beta]^{1/2}}{2 \times 3^{3/4}\beta}. \quad (1.42)$$

As the integration advances toward  $O$ , the step size is progressively decreased. The integration is continued until the ratio  $v/u$  converges to the desired accuracy. Table 1.1 shows  $E$  for a few values of  $\alpha$ .

Table 1.1. Relation of $\alpha$ and $E$	
$\alpha$	$E$
0	$-(\sqrt{3}/2)^{1/2} = -0.930605$
1	-1.095792
2	-1.161379
4	-1.218874
10	-1.270011

**Direction Field When  $0 > \alpha > -2$  ( $\frac{4}{3} > \beta > 0$ ).** When  $\beta > 0$ , the quantity  $v^3 - \beta v$ , which appears in the numerator of Eq. (1.34), is positive in the interval  $0 > v > -\sqrt{\beta}$ . Thus, when  $\alpha > 0$ , the equation  $\alpha u^2 = v^3 - \beta v$  for the curve  $C_0$  has real solutions for  $u$  in this interval, as depicted in Fig. 1.1. When  $\alpha < 0$ , it

has no real solutions for  $u$  in the interval  $0 > v > -\sqrt{\beta}$ , so the direction field for  $0 > \alpha > -2$  must look qualitatively different from that for  $\alpha > 0$ .

Figure 1.2 shows the direction field when  $0 > \alpha > -2$ . Again, the curves  $C_0$  and  $C_\infty$  intersect in the singular points  $O$  and  $P: (2/3^{3/4}, -2/\sqrt{3})$ . The point  $P$  is a saddle point at which the two possible slopes are given by Eq. (1.42) and by Eq. (1.42) with the sign preceding the square root changed from plus to minus. Both of these slopes are negative; the more negative of the two, which is the one we want, is that given by Eq. (1.42) as it stands.

ORNL-DWG 89-2338 FED

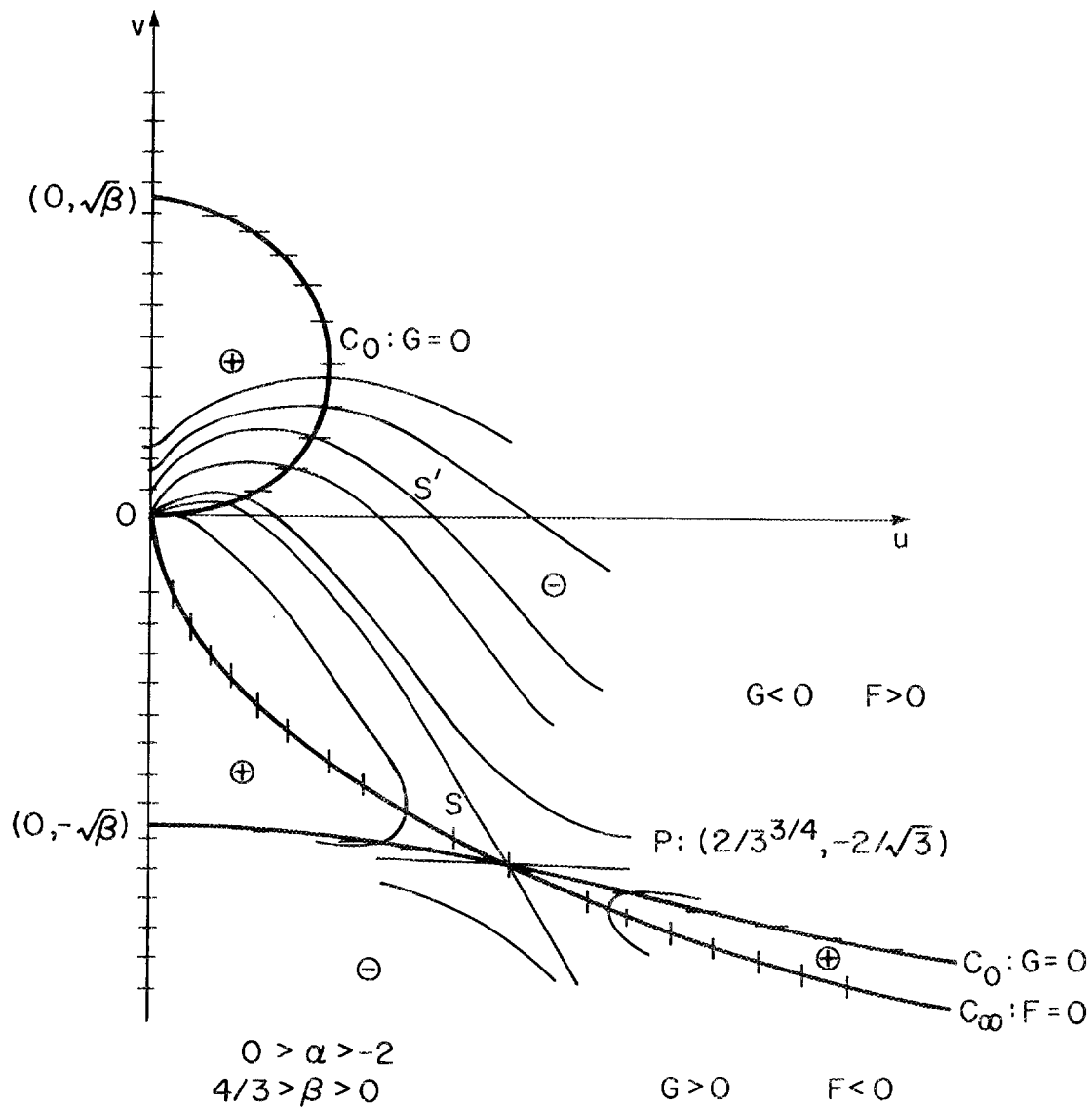


Fig. 1.2. The direction field of Eq. (1.34) with  $0 > \alpha > -2$ .

In Fig. 1.1, it is clear at a glance that all the integral curves in the lenticular region between  $C_0$  and  $C_\infty$  must pass through the origin. This conclusion applies, of course, to the separatrix  $S$ . In Fig. 1.2, the situation is slightly more complicated. Again, near  $O$ , there is the family of curves  $v = Eu$  passing through the origin. Again,  $E$  can have any value. In Fig. 1.1, only the curves having negative  $E$  are shown since only they lie in the lenticular region. In Fig. 1.2, we also consider curves with positive  $E$ . Besides this family of curves, there are two other curves that satisfy Eq. (1.34) to lowest order in  $u$  and  $v$ , namely,  $v = (\alpha/\beta)u^2$  and  $v = u^{2/3}$ . Neither of these was mentioned in connection with Fig. 1.1 because when  $\alpha > 0$  both lie in the first quadrant. Now, however, we need to consider them.

The direction field near  $O$  thus looks as shown in Fig. 1.2. The family  $v = Eu$  of rays through the origin is separated from integral curves that intersect the  $v$ -axis by a separatrix  $S'$ , which near the origin must behave like  $v = u^{2/3}$ , there being no other possibility. [Remember that  $v = (\alpha/\beta)u^2$  now lies in the fourth quadrant!] I have shown the separatrix  $S$  through  $P$  entering the origin with a positive slope  $E$ . We may expect the slope  $E$  to be positive for  $\alpha < -1$  since for  $\alpha > 0$  it is negative and for  $\alpha = -1$  it is zero. [The exact solution (1.29) for  $\alpha = -1$  can be written in terms of  $u = xy^{1/2}$  and  $v = x\dot{y}^{1/3}$  as  $v = -(3/2)u^2 = (\alpha/\beta)u^2$ . Thus,  $(dv/du)_O = 0$ .] Rule (1.37) now can be used to show that along the separatrix  $S$ ,  $O$  corresponds to  $x = 0$  and  $P$  corresponds to  $x = \infty$ . Continuation of the numerical calculations that led to Table 1.1 now yields the results given in Table 1.2. Shown in Fig. 1.3 is a graph of  $-E$  vs  $\alpha$  based on these numerical results.

Table 1.2. Relation of  $\alpha$  and  $E$  for negative values of  $\alpha$

$\alpha$	$E$
-0.5	-0.699404
-1.0	0
-1.1	0.276865
-1.25	0.870506
-1.40	2.848246
-1.42	5.487496

One consequence of these results is that when  $-2 < \alpha < -1$ , that is, when  $-\infty < \frac{\alpha}{\beta} < -\frac{3}{2}$ ,  $\dot{y}(0) > 0$  and  $y(x)$ , instead of being monotone decreasing on the interval  $0 < x < \infty$ , has a maximum for some  $x > 0$ .

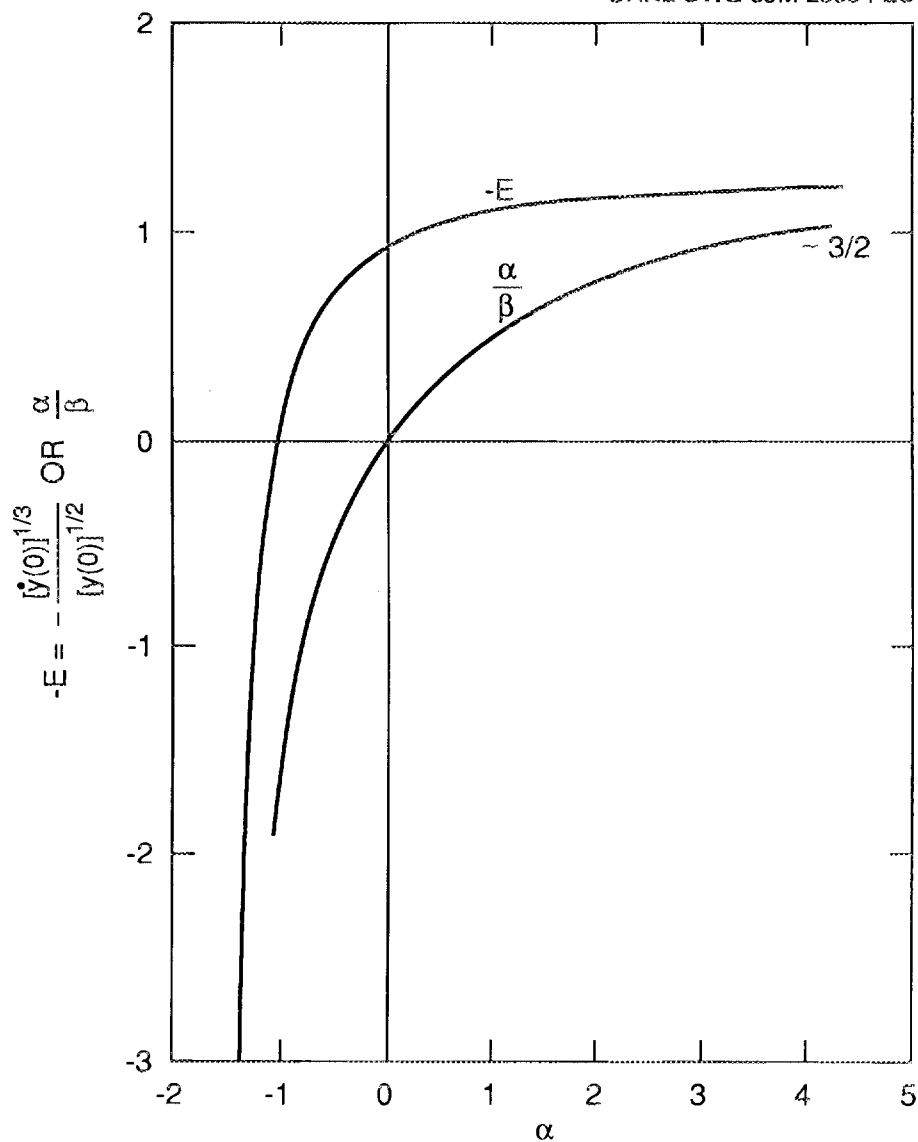


Fig. 1.3. The negative slope  $-E$  and the ratio  $\alpha/\beta$  plotted vs  $\alpha$ .

**Integration of the Differential Equation for  $y(x)$ .** The boundary conditions (1.10) supply boundary conditions at two different points, while a numerical integration of Eq. (1.19) requires two conditions at one point. Having calculated  $E$ , we know  $y(0)$  and  $\dot{y}(0)$  simultaneously and so can proceed with a numerical integration. Unfortunately, integration in the direction of increasing  $x$  is unstable, as trial quickly demonstrates. This instability occurs because integration in the direction

of increasing  $x$  is equivalent to traversing the separatrix  $S$  in the direction from  $O$  to  $P$ , that is, in the direction of diverging integral curves. Any small error, such as the truncation or roundoff error, throws us slightly off the separatrix  $S$ . When the integral curves diverge, as they do at a saddle point, the computed points eventually veer uncontrollably to one side of  $S$  or the other.

The instability does not affect the calculated points for small  $x$  very much, so we can join these points graphically to the known asymptotic behavior  $4/3\sqrt{3}x^2$ . Such a procedure can be successful in providing a rough picture of the function  $y(x)$ , but for high accuracy we must proceed otherwise.

What we need are the two boundary values  $y(x)$  and  $\dot{y}(x)$  at some large  $x$  so that we can integrate in the stable direction of decreasing  $x$ . One way to find such boundary values is as follows. First we find a point  $P' : (u, v)$  on the separatrix  $S$  close to  $P$ . It is simplest to use a point  $P'$  close enough to  $P$  that the coordinates of  $P'$  can be found from those of  $P$  by linear extrapolation using the slope  $m$  given in Eq. (1.42). Then we choose a value of  $x$  *arbitrarily* and calculate  $y$  and  $\dot{y}$  from the relations  $y = (u/x)^2$ ,  $\dot{y} = (v/x)^3$ . Using  $x$ ,  $y$ , and  $\dot{y}$  as initial data, we then integrate in the stable direction of decreasing  $x$ .

In general, this integration will produce an integral curve for which  $y(0) \neq 1$ . Now if we should happen to want the curve for which  $y(0) = 1$ , we can produce it by scaling our numerically calculated results with the transformation (1.8) for which  $\mu = [y(0)]^{-M/L} = [y(0)]^{1/2}$ . Then  $y'(0) = 1$ . The curves in Fig. 1.4 corresponding to  $\alpha = -5/4$  and  $\alpha = 1$  were calculated in this way. [The curves corresponding to  $\alpha = -1$  and  $\alpha = 0$  were calculated using appropriate versions of Eqs. (1.29) and (1.21).] Shown also for comparison is the common asymptotic limit  $y = 4/3\sqrt{3}x^2$ .

The reason this procedure works is as follows. Suppose we continue to denote by  $y'$  the integral curve that we seek. For some large  $x$ , say  $x = x_*$ ,  $y'$  will have the value  $y_*$  and  $\dot{y}'$  will have the value  $\dot{y}_*$ . If  $x_*$  is large enough,  $u = x_*y_*^{1/2}$  and  $v = x_*\dot{y}_*^{1/3}$  will be the coordinates of a point on  $S$  near  $P$ . Let  $y$  be an image of  $y'$  under the transformation (1.8); then  $y = \mu^{-2}y_*$ ,  $\dot{y} = \mu^{-3}\dot{y}_*$ , and  $x = \mu x_*$  are values of  $y$  and  $\dot{y}$  at some point  $x$  corresponding to the same values of  $u$  and  $v$  as given by  $u = x_*y_*^{1/2}$  and  $v = x_*\dot{y}_*^{1/3}$ . Since  $\mu$  can have any value,  $x$  can be made to assume any value. Thus, any  $x$  together with the coordinates  $(u, v)$  of a point  $P'$  on  $S$  yields consistent initial values  $x$ ,  $y$ ,  $\dot{y}$ .

**Further Discussion of the Similarity Solutions.** If we refer back to the direction field in Fig. 1.1, we may note that the integral curves which emanate from

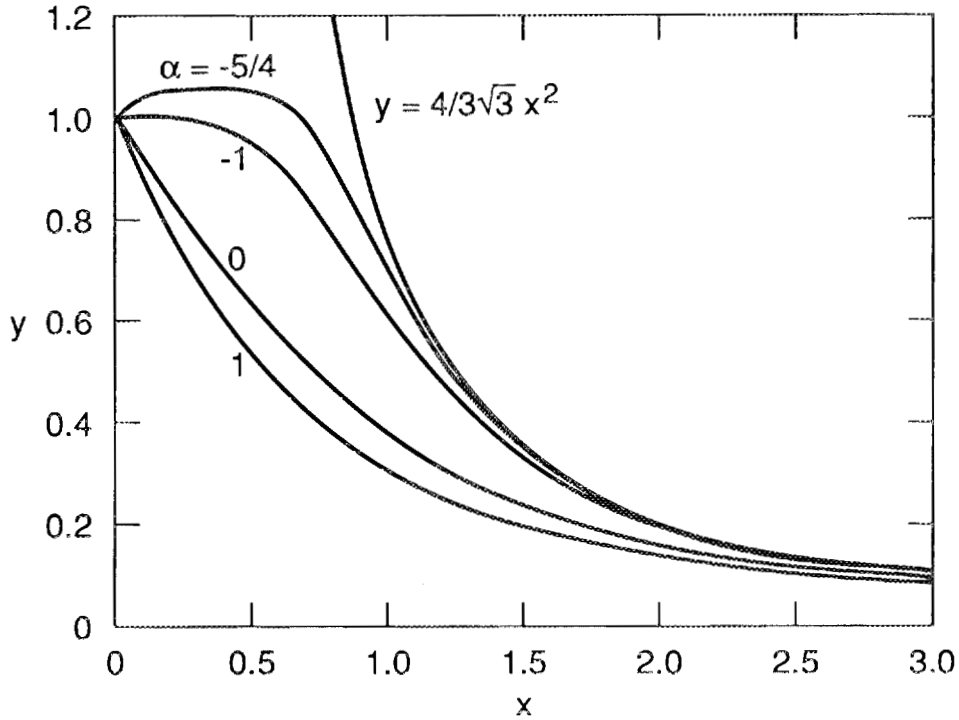


Fig. 1.4. Curves of  $y(x)$  plotted vs  $x$  for various  $\alpha$ . Also shown is the asymptotic limit  $y = 4/3\sqrt{3}x^2$ .

the origin  $O$  and lie below the separatrix  $S$  must eventually intersect the  $v$ -axis a second time at a point we denote by  $Q$ . Let  $v_0$  be the ordinate of  $Q$ . If, following the argument just given above, we choose an arbitrary value of  $x$ , say  $x_0$ , then  $Q$  corresponds to the consistent set of values  $x = x_0$ ,  $y = 0$ ,  $\dot{y} = (v_0/x_0)^3$ . If we integrate from  $Q$  to  $O$  we obtain a well-behaved solution  $y(x)$  on the interval  $0 < x < x_0$ . If for  $x > x_0$  we take  $y = 0$ , can we not thereby satisfy the boundary condition  $y(\infty) = 0$  and so obtain a satisfactory solution? After all, such segmented solutions are known for other diffusion-like partial differential equations—see, for example, the work of Pattle.<sup>2</sup>

The criterion for the admissibility of segmented solutions is that the two segments should obey the condition of conservation of heat at their intersection. We can derive this condition with the aid of Fig. 1.5. Let  $A$  be the position ( $z$ -coordinate) of the front  $y = T = 0$  at time  $t$  and let  $B$  be its position at time  $t + dt$ . The distance from  $A$  to  $B$  is  $Vdt$ , where  $V$  is the average velocity of the front in the interval  $dt$ .

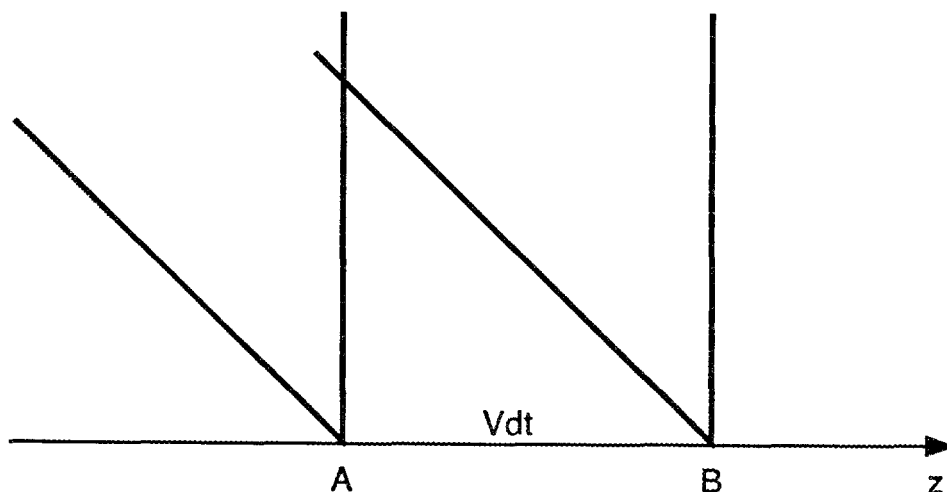


Fig. 1.5. The foot of the temperature distribution at time  $t$  and  $t + dt$ .

The oblique lines emanating from  $A$  and  $B$  represent the tail of the instantaneous temperature distributions  $T(z)$  at times  $t$  and  $t + dt$ . To lowest order, they are parallel. The heat crossing the point  $A$  into  $AB$  during  $dt$  is then  $\frac{1}{V} \int_0^{V dt} q(u) du$ , where  $u$  is the distance from the foot of the temperature distribution measured in the direction opposite to  $z$ . The average temperature rise in  $AB$  at the end of  $dt$  is  $\frac{1}{V dt} \int_0^{V dt} T(u) du$ . The heat capacity of  $AB$  is  $SV dt$ . Therefore, the condition of heat conservation reads

$$\frac{1}{V} \int_0^{V dt} q(u) du = S \int_0^{V dt} T(u) du . \quad (1.43)$$

Because Eq. (1.43) is an identity in  $V dt$ , differentiation with respect to the upper limit of the integrals yields

$$q(u) = SV T(u) . \quad (1.44)$$

Now for the superfluid diffusion equation,  $q(u) = K(dT/du)^{1/3}$ ; it therefore follows from Eq. (1.44) that  $\dot{T} = (SV/K)^3 T^3$ , which cannot be satisfied by a temperature distribution that falls to zero at the head of an advancing wave ( $u = 0$ ).

In Pattle's work,  $q = kT^m(dT/du)$ ; thus Eq. (1.44) becomes  $T^{m-1}\dot{T} = SV/k$ , which leads to  $T = (mSVu/k)^{1/m}$ . This relation admits segmented solutions. Furthermore, Pattle's explicit solutions satisfy it. So while in Pattle's case the segmented solution is admissible, it is not admissible for the superfluid diffusion equation.



## CHAPTER 2

### APPLICATIONS OF SIMILARITY SOLUTIONS

**Introduction.** Of the similarity solutions presented in Chap. 1, three are especially important: that to the clamped-temperature problem ( $\alpha = 0$ ), that to the clamped-flux problem ( $\alpha = 1$ ), and that to the pulsed-source problem ( $\alpha = -1$ ). The first of these is important because it has been made the basis of a theory of stabilization of superconductors by helium-II. The second and third are important because the problems that they solve have been studied experimentally.

The one-dimensional clamped-flux and pulsed-source problems can be studied by placing an electrical heater in a long tube filled with helium-II. The clamped-flux or pulsed-source boundary condition is then obtained by either holding the heater power fixed or pulsing it briefly. Such experiments have been performed by van Sciver<sup>3</sup> and by van Sciver and Lottin.<sup>4</sup> The clamped-temperature boundary condition can be visualized as resulting from the sudden contact of the end of the helium-filled tube with a large heat bath. The heat bath must be large so that the transfer of heat from the bath to the helium will not appreciably reduce the temperature of the heat bath; if the heat bath is too small, its temperature will decrease during the course of the experiment. However, owing to some peculiarities of the physical properties of helium, as long as the temperature of the heat bath is high enough, even if it changes during the experiment, the flow of heat down the tube will be very close to what it would be if the temperature of the heat bath were clamped at the He-I-He-II transition temperature  $T_\lambda$  ( $\sim 2.17$  K).

To see how this comes about, we need to fix in our minds the phase diagram of helium at low temperatures (Fig. 2.1). The ordinate is pressure, the abscissa temperature. The curve  $OC$  is the saturation curve that separates liquid on the left from vapor on the right. The point  $C$  is the critical point, beyond which no distinction between vapor and liquid is possible. Rising almost vertically from the point  $\lambda$  on the saturation curve is the line that separates He-II on the left from ordinary He-I on the right. The point  $\lambda$  is called the lambda point, and the nearly vertical line, the lambda line. Shown in the He-II region is the point  $P$  at  $T = 1.8$  K and pressure  $P = 1$  atm. This point is a typical operating point when He-II is used as a coolant in technical applications.

If the temperature of the heat bath is high enough, the helium immediately in contact with the heat bath will have a temperature higher than that of the lambda

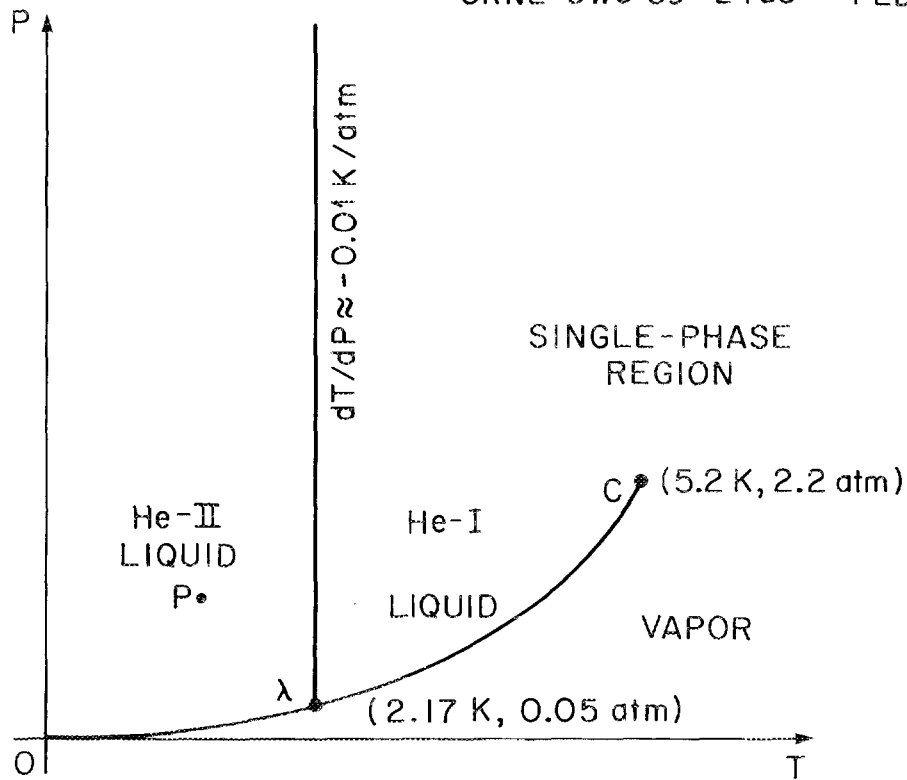


Fig. 2.1. The phase diagram of helium.

line. (The pressure in the tube is assumed uniform.) Thus a layer of liquid He-I (and possibly a layer of vapor) will separate the heat bath and the bulk of the He-II. The downstream boundary of this He-I layer has the temperature of the lambda line (approximately  $T_\lambda$ ). In most practical situations, the heat flux  $Q$  down the tube (and thus across the He-I layer) is a few watts per square centimeter; the temperature difference  $\Delta T$  between the solid and the helium in the tube is a few kelvins. The thickness  $\delta$  of the He-I layer is approximately  $k\Delta T/Q$ , where  $k$  is the thermal conductivity of He-I ( $\sim 10^{-4} \text{ W}\cdot\text{cm}^{-1}\cdot\text{K}^{-1}$ ). Owing to the smallness of  $k$ ,  $\delta$  is of the order of  $10^{-4} \text{ cm}$ . Thus the He-I-He-II interface, at which  $T = T_\lambda$ , is always very close to the surface of the heat bath. Such a thin layer also has an extremely small heat capacity ( $\sim 40 \mu\text{J}\cdot\text{cm}^{-2}\cdot\text{K}^{-1}$ ), and so its thickness can respond to changes in the heat flux through it in times of the order of tens of microseconds. Looking back from the He-II-filled tube at the heat bath, one thus sees a surface on which the temperature is clamped at  $T = T_\lambda$  and whose location is, for all practical purposes, identical with that of the heat bath. The temperature distribution in the

tube and the heat flow down the tube are then well approximated by the solution of the clamped-temperature problem with  $T(0, t) = T_\lambda$ . This extremely important observation was first made by Seyfert, Lafferandierie, and Claudet,<sup>5</sup> who summarized the situation succinctly as follows: “At the onset of burnout [transition from He-II to He-I at the surface of the heat bath], formation of the thermal barrier starts. The He-II near the heated surface experiences a phase transition. A He-II–He-I interface appears which has its temperature locked at  $T_\lambda$  . . . . We assumed that this barrier has a negligible thickness and that it only affected heat transport in He-II by the condition of a constant temperature, i.e.,  $T = T_\lambda$ , at the hot end of the channels in our test section.”

The observation of Seyfert et al. has made it possible to base a theory of stabilization of superconductors by He-II on the solution to the clamped-temperature problem, and this theory is described in the next section. The solution to the clamped-temperature problem can also be made the basis of a theory of bubble growth in superheated He-II. This theory is described here, too. Next, after a brief comparison with the experimental results of van Sciver and Lottin, the solution of the pulsed-source problem is used to analyze the pulsed time-of-flight method of measuring flow velocity. Then the solution to the clamped-flux problem is briefly compared to the experimental results of van Sciver. This solution is made the basis of an approximate solution of the problem in which the heat flux into the tube is imposed by an external agency but not held constant. Experiments of this sort have been performed by Okamura et al.<sup>6</sup> Finally, a similarity solution to the clamped-temperature problem valid in the temperature range  $1.9 \text{ K} < T < T_\lambda$  is presented for the case in which  $K$  and  $S$  are not constant but have their real variations with temperature.

**Stabilization of Superconductors.** We begin by assuming the thermophysical properties  $K$  and  $S$  to be constant, as in Chap. 1. Because  $K$  and  $S$  both vary strongly with temperature near  $T_\lambda$ , the criterion for stability that we derive below on the basis of constant  $K$  and  $S$  may be inaccurate. In the last section of this chapter, we estimate the degree of this inaccuracy. But for the time being, we take  $K$  and  $S$  to be constant.

We consider a superconductor cooled by contact with a closed channel of length  $L$  filled with He-II (see Fig. 2.2). The thermodynamic state of the He-II is that denoted by a point in the phase diagram like point  $P$  in Fig. 2.1 ( $T = T_b$ ). Suppose the superconductor is driven normal (i.e., nonsuperconducting) by a sudden heat

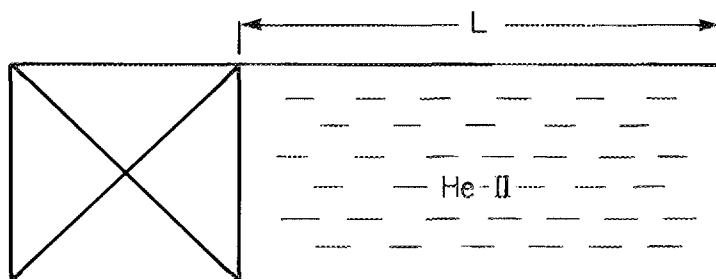


Fig. 2.2. Schematic diagram of a superconductor cooled by contact with a closed channel of length  $L$  filled with He-II.

pulse  $E$ , after which it produces a steady Joule power  $q_J$ . (The quantities  $E$  and  $q_J$  are both expressed per unit area of wetted surface and therefore have SI units of  $\text{J}\cdot\text{m}^{-2}$  and  $\text{W}\cdot\text{m}^{-2}$ , respectively.) If  $E$  is small enough, the He-II cools the superconductor well enough to overcome the Joule heating, and the superconductor returns to the superconducting state. If  $E$  is too large, the Joule heating overwhelms the cooling by He-II, and the superconductor does not return to the superconducting state. We seek the largest value of  $E$  for which the superconductor can still recover the superconducting state.

Seyfert et al.<sup>5</sup> have given a simple method of calculating  $E$  based on the balance of areas shown in Fig. 2.3. In this diagram, the ordinate is the heat flux from the conductor into the helium through the wetted surface and the abscissa is the time elapsed since the beginning of the heat pulse  $E$ . The stepped curve depicts the power production in the superconductor. The initial heat pulse  $E$ , shown having a duration  $t_1$ , is the first part of this stepped curve. After the time  $t_1$  elapses, the superconductor is assumed to have been driven normal and to be producing a steady Joule power  $q_J$ . The part of the stepped curve depicting this Joule power production is labeled “post-heating.”

The smooth curve labeled “similarity solution” represents the heat flux  $q$  into the He-II through the surface at which  $T = T_\lambda$ . This curve, whose equation we shall calculate later, is a decreasing function of time. At the time  $t_2$ , it crosses the level  $q_J$  of the post-heating flux. If, by the time  $t_2$ , the helium has not withdrawn all of the heat produced in the superconductor, the superconductor will not have cooled enough to regain the resistanceless superconducting state. Then Joule heat

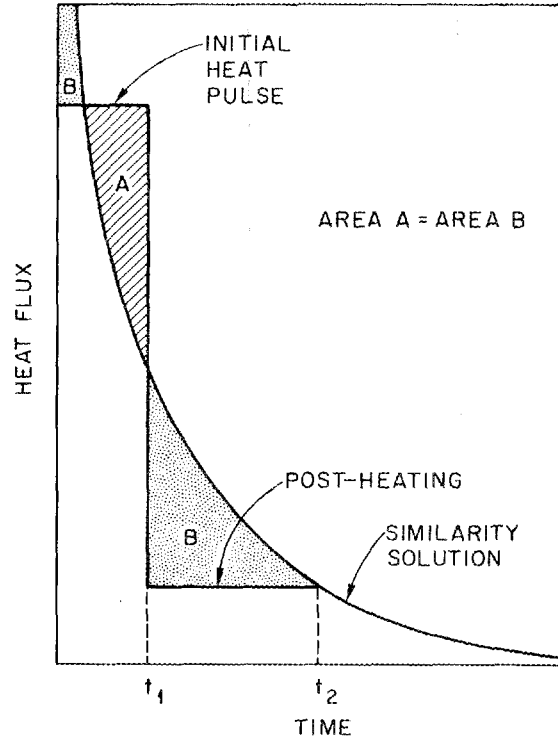


Fig. 2.3. Sketch depicting the balance-of-areas argument of Seyfert et al.<sup>5</sup>

production at the steady level  $q_J$  will persist beyond  $t_2$ , where it will exceed the cooling  $q$  of the helium. But then the conductor, being heated more strongly than cooled, will never regain the superconducting state. From this reasoning, it is clear that the largest value of  $E$  corresponds to the condition that all the heat produced in the superconductor up to time  $t_2$  must just equal the heat withdrawn by the helium. This means that, in Fig. 2.3, the areas from  $t = 0$  to  $t = t_2$  under the stepped and smooth curves must be equal; equivalently, area  $A$  must equal area  $B$ .

If the channel is long enough, recovery of the superconducting state takes place before much heat has reached the far end of the cooling channel. Then from the near end, the channel looks infinitely long. According to Seyfert et al., the channel can thus be treated as a semi-infinite tube, the temperature of whose front surface ( $z = 0$ ) is suddenly ( $t = 0$ ) clamped at  $T_\lambda$ . It then follows from the solution (1.24a) and (1.25) to the clamped-temperature problem that

$$q = -K \left( \frac{\partial T}{\partial z} \right)_{z=0}^{1/3} = \left( \frac{\sqrt{3}}{2} \right)^{1/2} K^{3/4} S^{1/4} (T_\lambda - T_b)^{1/2} t^{-1/4} \equiv B t^{-1/4}. \quad (2.1)$$

The constant  $A$  in Eqs. (1.24) and (1.25) that represents the clamped-temperature rise of the surface  $z = 0$  has been replaced by  $T_\lambda - T_b$ , the difference between the lambda temperature and the temperature  $T_b$  of the ambient helium (point  $P$  in Fig. 2.1). The balance of areas can now be written as

$$\int_0^{t_2} q dt = E + q_J(t_2 - t_1) , \quad (2.2)$$

where  $t_2$  is given by

$$t_2 = (B/q_J)^4 . \quad (2.3)$$

If in Eq. (2.2) we assume that  $t_2 \gg t_1$ , then we find that

$$E = \frac{1}{3} q_J t_2 , \quad (2.4a)$$

$$t_2 = \frac{3}{4} K^3 S (T_\lambda - T_b)^2 q_J^{-4} , \quad (2.4b)$$

so that

$$E = \frac{1}{4} K^3 S (T_\lambda - T_b)^2 q_J^{-3} . \quad (2.4c)$$

If the channel is short enough, the characteristic time for the temperature distribution in the channel to approach uniformity is short compared with the time it takes to regain the superconducting state. Then all of the enthalpy of the helium is available for recovery, and

$$E = [h(T_\lambda) - h(T_b)] L \equiv E_0 , \quad (2.5)$$

where  $h(T)$  is the enthalpy per unit volume of helium. If we consider  $E/E_0$  as a function of  $q_J/q_*$ , where

$$q_* = K S^{1/3} (T_\lambda - T_b)^{2/3} (4E_0)^{-1/3} , \quad (2.6)$$

we can combine Eqs. (2.4c) and (2.5) as follows:

$$\frac{E}{E_0} = \begin{cases} 1 , & q_J/q_* \ll 1 \\ (q_J/q_*)^{-3} , & q_J/q_* \gg 1 \end{cases} . \quad (2.7a)$$

$$(2.7b)$$

The author has made the two limits (2.7a) and (2.7b) the basis of a practical theory of superconductor stability.<sup>7</sup> This theory requires some additional elaboration that is not described here because that would carry us too far afield of our general goal of studying the mathematics of the superfluid diffusion equation. The reader

seeking these details may consult refs. 2–7 as well as the confirmatory experimental studies of Pfothenhauer and van Sciver.<sup>8</sup>

**Bubble Growth in Superheated He-II.** Suppose we have a sample of He-II at a pressure  $P$  and a temperature  $T_b = T_S(P) + \Delta T$ , where  $T_S(P)$  is the saturation temperature corresponding to the pressure  $P$  and  $\Delta T$  is a small superheat. Such a sample is thermodynamically unstable and tends to change into vapor. The rate of this conversion depends on the density of nucleation sites initially present and the rate of growth of the bubbles arising at these sites.

The rate of bubble growth is controlled by the transfer of heat from the superheated liquid to the surface of the growing bubble. In He-II, this heat transfer is controlled by the superfluid heat conduction process described by Eqs. (1.1) and (1.2).

Again the procedure is to consider limiting cases. When the superheat  $\Delta T$  is very small, bubble growth is slow and the temperature distribution in the liquid surrounding a bubble will be very close to the steady-state distribution  $T = T_b - \Delta T R^5 / r^5$ , where  $R$  is the instantaneous bubble radius and  $r$  ( $> R$ ) is the radial coordinate measured from the center of the bubble. This temperature distribution is a steady-state ( $T_t = 0$ ) solution of Eq. (1.3), as can be verified by substitution. When the superheat  $\Delta T$  is very large, bubble growth is rapid and the temperature distribution in the liquid is never close to the steady-state distribution. We can approximate it with the help of the assumption, justified later, that the layer in which the temperature changes is thin compared with the radius of the bubble. There we can neglect the curvature of that layer. The temperature distribution in that layer in a coordinate system moving with the bubble surface is then given by the solution to the clamped-temperature problem with the  $z = 0$  surface (the bubble surface) clamped at the saturation temperature  $T_S$ . Since  $T_S = T_b - \Delta T < T_b$ , the clamped-temperature rise at  $z = 0$ ,  $T_S - T_b$ , is actually negative ( $-\Delta T$ ). This requires some small changes in Eqs. (1.24) and (1.25) which can best be determined by repeating the derivation leading from Eq. (1.19) to Eq. (1.24). These changes require that the sign of the right-hand side of Eq. (1.20) be changed and that  $A$  be set equal to  $-\Delta T$  in Eq. (1.24a) and  $\Delta T$  in Eqs. (1.24b) and (1.25).

In the first case, when the superheat is small, the *inward* heat flux at the bubble surface is

$$K \left( \frac{\partial T}{\partial r} \right)_{r=R}^{1/3} = K (5\Delta T/R)^{1/3} . \quad (2.8)$$

The quasistatic heat balance for the growing bubble is then

$$4\pi R^2 \dot{R} \rho_v L = 4\pi R^2 K (5\Delta T/R)^{1/3} , \quad (2.9)$$

where  $\rho_v$  is the density of the vapor in the bubble and  $L$  is the latent heat of vaporization of helium. Equation (2.9) is easily integrated and yields

$$R = \left(\frac{4}{3}\right)^{3/4} 5^{1/4} \left(\frac{Kt}{\rho_v L}\right)^{3/4} (\Delta T)^{1/4} \quad (\text{small superheat}) . \quad (2.10)$$

In the second case, when the superheat is large, the inward heat flux through the bubble surface can be calculated from Eqs. (1.24) and (1.25):

$$K \left(\frac{\partial T}{\partial z}\right)_{z=0}^{1/3} = \left(\frac{\sqrt{3}}{2}\right)^{1/2} K^{3/4} S^{1/4} (\Delta T)^{1/2} t^{-1/4} . \quad (2.11)$$

Now the heat balance for the growing bubble is

$$4\pi R^2 \dot{R} \rho_v L = 4\pi R^2 \left(\frac{\sqrt{3}}{2}\right)^{1/2} K^{3/4} S^{1/4} (\Delta T)^{1/2} t^{-1/4} . \quad (2.12)$$

Equation (2.12) is also easily integrated and yields

$$R = \left(\frac{8}{3\sqrt{3}}\right)^{1/2} \left(\frac{Kt}{\rho_v L}\right)^{3/4} (\Delta T)^{1/4} \left(\frac{S\Delta T}{\rho_v L}\right)^{1/4} \quad (\text{large superheat}) . \quad (2.13)$$

A comparison of Eqs. (2.10) and (2.13) shows that, except for a minor difference in the numerical constant, they differ in the appearance of the factor  $(S\Delta T/\rho_v L)^{1/4}$ . When this factor is very small, the radius given by Eq. (2.13) is much less than that given by Eq. (2.10), so we must use the radius of Eq. (2.10). When  $(S\Delta T/\rho_v L)^{1/4} \gg 1$ , the radius of Eq. (2.13) is much larger than that of Eq. (2.10), and we must use the radius of Eq. (2.13). The break in use between these two equations comes at superheats of the order of  $\rho_v L/S$  that make the factor  $(S\Delta T/\rho_v L)^{1/4}$  roughly 1.

The thickness of the temperature transition layer will be small compared with the radius given in Eq. (2.13) if the value of  $X$  in Eq. (1.25) calculated for  $z = R$  is large compared with 1. We find

$$X(R) = \left(\frac{8}{3\sqrt{3}}\right)^{1/2} \left(\frac{S\Delta T}{\rho_v L}\right) , \quad (2.14)$$

so again we find that the condition for the use of Eq. (2.13) is that  $S\Delta T/\rho_v L \gg 1$ .

An additional argument for the use of Eq. (2.10) when  $S\Delta T/\rho_v L \ll 1$  is this: The characteristic time to establish the steady-state temperature distribution  $T = T_b - \Delta T R^5/r^5$  is determined by the superfluid conductivity  $K$ , the superfluid heat capacity per unit volume  $S$ , the superheat  $\Delta T$ , and the bubble radius  $R$ . The only time that can be made out of these four quantities is  $\tau = S(\Delta T)^{2/3} R^{4/3} K^{-1}$ . The quasistatic theory is applicable when  $\dot{R}\tau \ll R$  for the  $R$  given by Eq. (2.10). We find after a short calculation that

$$\frac{\dot{R}\tau}{R} = 5^{1/3} \left( \frac{S\Delta T}{\rho_v L} \right), \quad (2.15)$$

which shows, as expected, that the condition for the use of Eq. (2.10) is that  $S\Delta T/\rho_v L \ll 1$ .

The theory presented here for bubble growth ignores the inertial reaction of the fluid as it is pushed away by the expanding bubble. This inertial reaction is considered in ref. 9, in which this theory was first published. But we shall not go into these details because what interests us here is the application of the similarity solutions of Chap. 1 to particular physical problems.

A related problem in which there is no displacement of the fluid by the vapor is that of evaporation from a free surface. A long tube containing liquid He-II is imagined to extend in the  $z$ -direction, and the initial position of the free surface is taken to be  $z = 0$ . At  $t = 0$ , the pressure above the free surface is dropped suddenly so that the liquid, at temperature  $T_b$ , becomes superheated by an amount  $\Delta T$ . The vapor produced at the free surface exhausts in the negative  $z$ -direction, while the free surface  $z = Z(t)$  advances in the positive  $z$ -direction.

Early enough, the tube can be treated as infinitely long. The boundary and initial conditions are then

$$T(z, 0) = T_b, \quad (2.16a)$$

$$T(\infty, t) = T_b, \quad (2.16b)$$

$$T(Z(t), t) = T_S, \quad (2.16c)$$

$$\rho_\ell L \dot{Z} = K \left( \frac{\partial T}{\partial z} \right)_{z=Z}^{1/3}. \quad (2.16d)$$

The first two conditions state that the initial temperature and the temperature far down the tube are  $T_b$ . The third says that the liquid temperature at the free surface is the saturation temperature  $T_S = T_b - \Delta T$ . The fourth is a heat balance that

says that the heat transported to the surface by superfluid conduction is expended in vaporizing liquid.

We again make the assumption that  $K$  and  $S$  are independent of temperature and work in special units in which  $K = S = 1$ ; thus we must solve the version of the superfluid diffusion equation given by Eq. (1.4). Equations (1.4) and (2.16) have a similarity solution of the form

$$T_b - T = y \left( z/t^{3/4} \right) , \quad (2.17a)$$

$$Z = At^{3/4} , \quad (2.17b)$$

where  $A$  is a constant yet to be determined. Substitution of Eq. (2.17a) into Eq. (1.4) shows that  $y$  satisfies Eq. (1.19) with  $\alpha = 0$  and  $\beta = 4/3$ . The four boundary conditions (2.16) collapse to

$$y(\infty) = 0 , \quad (2.18a)$$

$$y(A) = \Delta T , \quad (2.18b)$$

$$\dot{y}^{1/3}(A) = - \left( \frac{3}{4} \right) \rho_\ell L A . \quad (2.18c)$$

We can use Eq. (1.20) for  $\dot{y}$  since  $y$  satisfies Eq. (1.19) with  $\alpha = 0$  and  $\beta = 4/3$ . If we substitute Eq. (1.20) into the boundary conditions (2.18), they become

$$\int_A^\infty \left( \frac{3}{4}x^2 + \frac{1}{a^2} \right)^{-3/2} dx = \Delta T \quad (2.19a)$$

and

$$\left( \frac{3}{4}A^2 + \frac{1}{a^2} \right)^{-1/2} = \frac{3}{4} \rho_\ell L A . \quad (2.19b)$$

Equations (2.19) can be used to calculate the constant  $A$ , which determines the displacement of the free surface as a function of time. The calculation is tedious and the result complicated except when  $S\Delta T/\rho_\ell L \ll 1$ , which is nearly always the case. In this limit, *in ordinary units*

$$Z = \left( \frac{8}{3\sqrt{3}} \right)^{1/2} \left( \frac{Kt}{\rho_\ell L} \right)^{3/4} (\Delta T)^{1/4} \left( \frac{S\Delta T}{\rho_\ell L} \right)^{1/4} , \quad (2.20)$$

which is precisely the same as Eq. (2.13) save that  $\rho_\ell$ , the liquid density, replaces  $\rho_v$ , the density of the vapor. Since the ratio of these densities is of the order of 1000, bubble growth velocities are three orders of magnitude greater than free surface velocities.

**The Pulsed-Source Problem and the Pulsed Time-of-Flight Method of Measuring Flow Velocity.** Lottin and van Sciver<sup>4</sup> have measured the temperature distribution in a long, 6-mm-diam, He-II filled tube after a 0.92-J heat pulse at its center ( $z = 0$ ). Their data are shown in Fig. 2.4. The inset shows their measured profiles of temperature rise at various times after the pulse. The main drawing shows a comparison of these same points with the similarity solution (1.31)

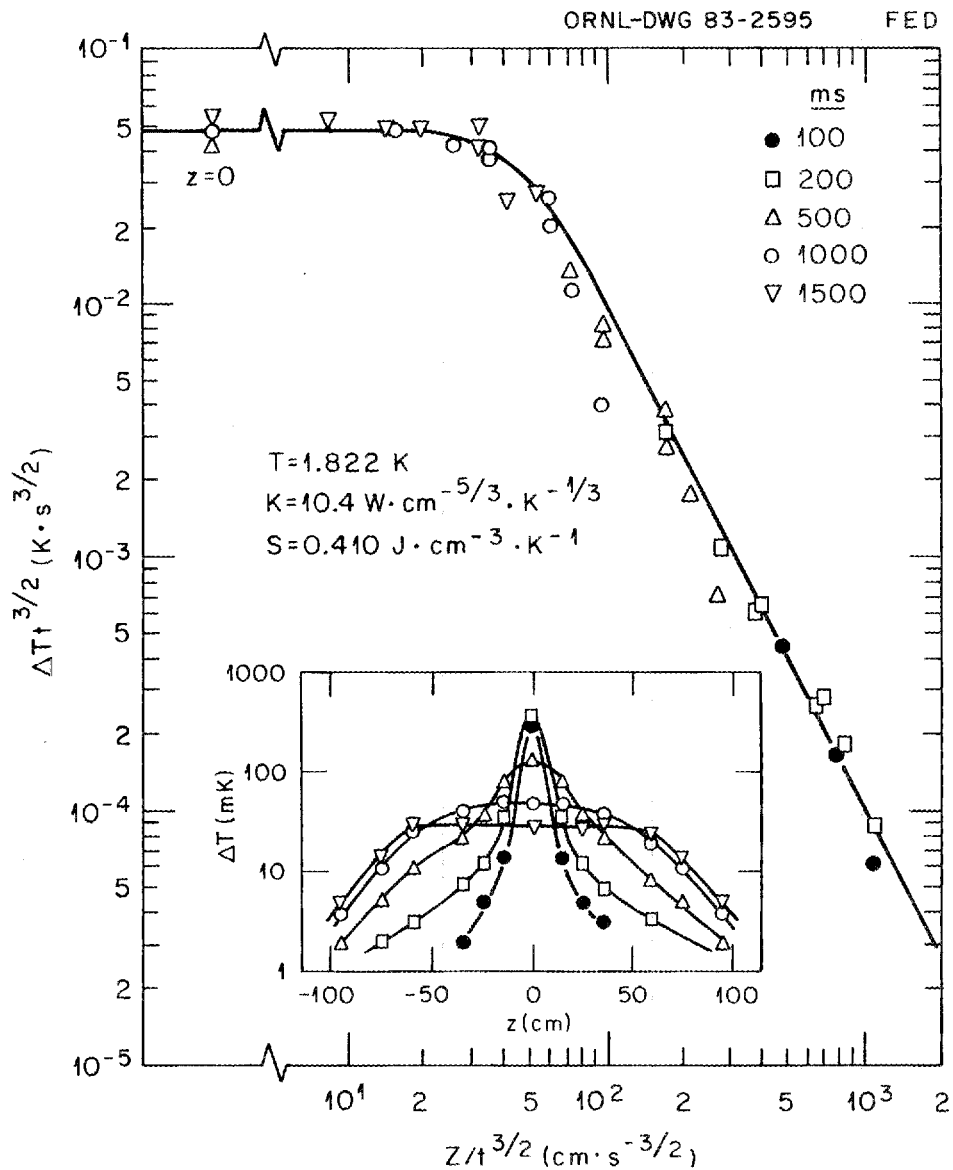


Fig. 2.4. The temperature distribution in a long, 6-mm-diam, He-II-filled tube after a 0.92-J heat pulse at its center, as measured by Lottin and van Sciver.<sup>4</sup> The curve is the similarity solution (1.31) and (1.32).

and (1.32). Here  $K$  and  $S$  have been given their measured values at 1.8 K (ref. 10). The agreement of theory and experiment is excellent.

The solution to the pulsed-source problem can be used to study the effectiveness of the time-of-flight method of measuring flow velocity in a pipe. A short pulse of heat is injected into the fluid at one point, and its time of arrival at a second point is measured. Because the heat pulse may spread owing to conduction (molecular or turbulent), a convenient time to measure is that corresponding to the arrival at the second point of the maximum temperature.

In principle, even if there were no flow at all, the temperature recorded at the second point would have a maximum. In ordinary fluids, the arrival time of this no-flow maximum is so long that it can easily be distinguished from the much shorter arrival times caused by flow. So axial conduction causes no practical problem in ordinary fluids.

In He-II, on the other hand, axial heat transport by superfluid conduction is very large. Because of the rapid spread of the temperature distribution it causes, the arrival time of the maximum temperature for low flow velocities may not be very different from that in the no-flow case. The accuracy with which the arrival time can be determined then sets a lower limit to the flow velocity that can reliably be measured. Because an analytic solution to the pulsed-source problem in He-II is known, these considerations can be quantified as shown below.

The temperature distribution in the moving fluid is governed by the partial differential equation

$$ST_t = \left(KT_z^{1/3}\right)_z - vST_z. \quad (2.21)$$

The last term in Eq. (2.21) accounts for the convective transfer of heat downstream. As before, we assume that  $K$  and  $S$  are constant, work in special units in which  $K = S = 1$ , and interpret  $T$  as the temperature rise. The boundary and initial conditions are exactly those of the pulsed-source problem, namely,  $T(z, 0) = 0$ ,  $T(\pm\infty, t) = 0$ , and  $\int_{-\infty}^{+\infty} T dz = Q$ . For convenience, we further specialize our system of special units by taking  $Q = v = 1$ . No additional quantities may be set equal to 1.

The solution we seek is given by Eqs. (1.31) and (1.32) with  $z$  replaced in Eq. (1.32) by  $z - vt$  ( $= z - t$  in special units):

$$T = \frac{4}{3\sqrt{3}} \left[ (z - t)^4 t^{-3} + b^4 t^3 \right]^{-1/2}. \quad (2.22)$$

The maximum value of  $T$  (at some fixed  $z$ ) occurs when the bracketed quantity has its minimum. A short calculation shows that this occurs when  $z$  and  $t$  satisfy

$$z = xt_{\max}, \quad (2.23a)$$

$$(x-1)^3(3x+1) = 3b^4 t_{\max}^2, \quad (2.23b)$$

where  $x$  is an auxiliary variable. The simplest way to find  $t_{\max}$  as a function of  $z$  is to choose  $x$  and solve Eqs. (2.23a) and (2.23b) for  $z$  and  $t_{\max}$ . Figure 2.5 shows a plot constructed in this way of  $t_{\max}/z^{2/3}$  vs  $z$  (or, in ordinary units,  $Kt_{\max}/(z^2SQ^2)^{1/3}$  vs  $K^3z/(v^3SQ^2)$ ). Using such a plot, we can use measured values of the ordinate to find the corresponding value of the abscissa, which depends on  $v$ , and thus determine  $v$ .

When  $v$  is very small, the special units of length ( $v^3SQ^2/K^3$ ) and time ( $v^2SQ^2/K^3$ ) are small. Then  $t_{\max}$  in special units is very large and  $x$  is very large, too. In the limit of very small  $v$ , then, Eqs. (2.23a) and (2.23b) simplify to

$$t/z^{2/3} = b^{-2/3} = 0.4969466668\dots \quad (\text{special units; zero velocity}). \quad (2.24)$$

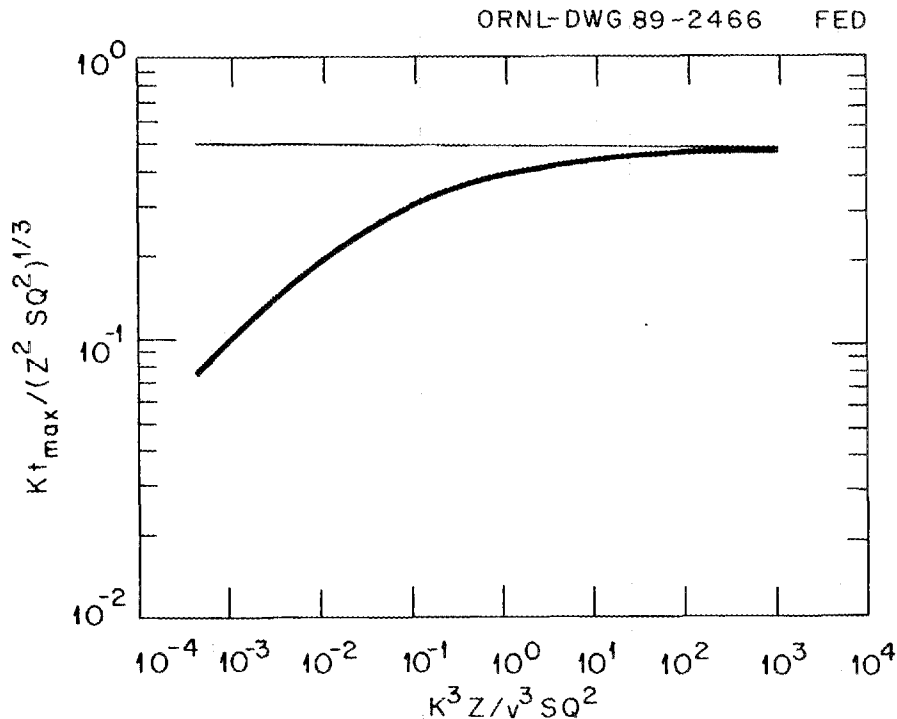


Fig. 2.5. A curve from which the flow velocity  $v$  may be determined from a measurement of  $t_{\max}$ , the time at which the temperature a distance  $Z$  from the source point reaches its maximum.

This value is shown as a horizontal straight line in Fig. 2.5. When the abscissa is large ( $v$  small), the curve asymptotically approaches this value from below, and thus its slope becomes ever smaller. This slope is easily calculated from Eqs. (2.23a) and (2.23b) and is given by

$$\frac{d \ln (t_{\max}/z^{2/3})}{d \ln z} = \frac{4x + 2}{3(9x^2 - 2x - 1)}. \quad (2.25)$$

The decrease in slope magnifies the fractional error in  $v$  compared with the fractional error in  $t_{\max}$ . For example, when  $z = 1000$ , the slope given in Eq. (2.25) is  $7.46 \times 10^{-3}$ . Since the abscissa in ordinary units is inversely proportional to  $v^3$ , the slope  $d \ln t_{\max}/d \ln v$  is three times as great. Thus, inverting, we find  $dv/v = 44.7 (dt_{\max}/t_{\max})$ , so that in this example, a 1% error in determining the arrival time of the temperature maximum results in a 45% error in the flow velocity  $v$ .

Suppose we consider helium at  $T_b = 1.8$  K and locate our thermometer 30 cm downstream of the heater. What is the smallest  $v$  we can successfully measure? To answer this question we must first decide what accuracy we seek in determining  $v$ . Suppose we want 1% accuracy. If  $d \ln v/d \ln t_{\max}$  is as large as 45, as it was in the illustration above, we would then have to determine the arrival time of the maximum with a fractional error no greater than  $2 \times 10^{-4}$ . This is a very small error and may not be attainable. Suppose we select an upper limit for  $d \ln v/d \ln t_{\max}$  of 3. Then, since Eq. (2.25) implies that

$$\frac{d \ln v}{d \ln t_{\max}} = \frac{9x^2 - 2x - 1}{4x + 2}, \quad (2.26)$$

we find that  $x < (7+4\sqrt{7})/9 = 1.954 \dots$ . Then from Eq. (2.23) it follows that  $t_{\max} < 0.1728$  and  $z < 0.3377$  in special units. In ordinary units this reads  $K^3 z/v^3 S Q^2 < 0.3377$ . If we take the value of  $Q$  to be that used by Lottin and van Sciver, we find that the lower limit to  $v$  in this example is about 30 cm/s. Trying to reduce this limit substantially by increasing  $Q$  may introduce another source of inaccuracy, namely, that caused by the temperature variation of the physical properties  $K$  and  $S$ . The analysis presented above is as far as we can go using the similarity solution (1.31) and (1.32).

**The Clamped-Flux Problem.** Figure 2.6 shows a comparison of temperature differences measured by van Sciver<sup>3</sup> with the similarity solution  $y(x)$  for  $\alpha = 1$  taken from Fig. 1.4. The physical properties  $K$  and  $S$  have been chosen to make the

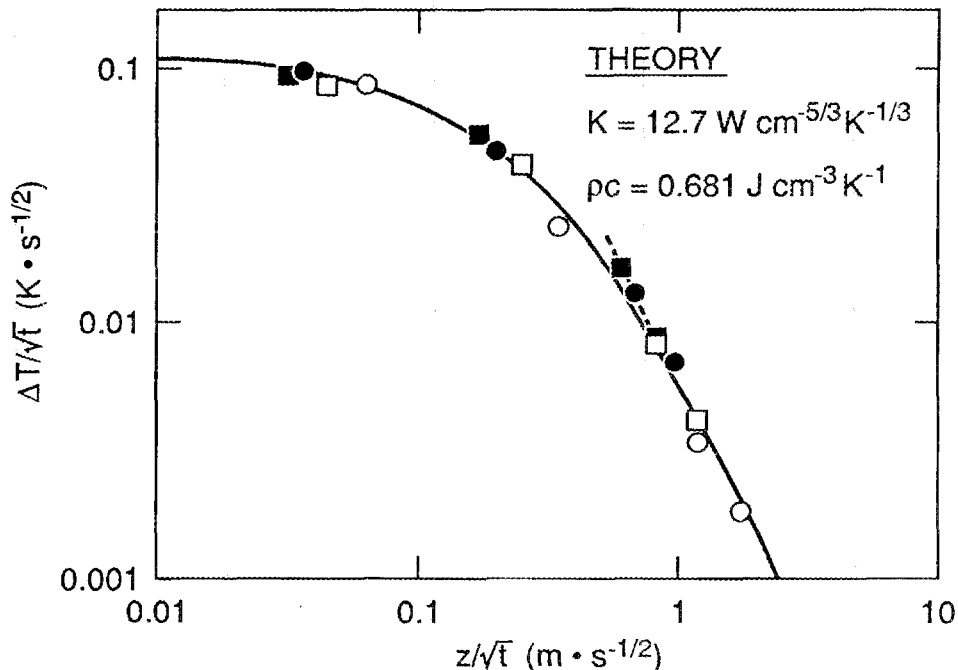


Fig. 2.6. A comparison of the temperature differences measured by van Sciver<sup>3</sup> in the clamped-flux case ( $\alpha = 1$ ) with the similarity solution  $y(x)$ .

similarity solution fit the experimental points as closely as possible.<sup>11</sup> The best-fit values differ somewhat from the point values at  $T_b = 1.8$  K given in Table 2.1,<sup>10</sup> the differences in  $K$  being slight and those in  $S$  more substantial. A possible reason for this is that van Sciver's measured temperature distributions spanned the range from 1.8 K to 2.0 K, in which  $K$  increases slightly but  $S$  nearly doubles. Similar differences do not occur in the case of Fig. 2.4, where the points span the much narrower temperature range 1.82–1.87 K.

Table 2.1. Thermophysical properties of He-II<sup>a</sup>

$T$ (K)	$K$ ( $\text{W}\cdot\text{cm}^{-5/3}\cdot\text{K}^{-1/3}$ )	$S$ ( $\text{J}\cdot\text{cm}^{-3}\cdot\text{K}^{-1}$ )
1.8	10.4	0.410
1.9	11.6	0.553
2.0	11.6	0.756
2.1	8.35	1.10

<sup>a</sup>Values from ref. 10.

Whereas van Sciver used steady heat flux, thus conforming to the conditions of applicability of the clamped-flux solution, Okamura et al.<sup>6</sup> imposed a sinusoidal time variation on the heat flux into the helium. The remainder of this section is devoted to explaining the use of similarity solutions as a jumping-off point for an approximate treatment of such a problem as Okamura's.

We still wish to find solutions of Eq. (1.4) satisfying the first two boundary conditions of Eq. (1.9). The last boundary condition no longer applies, and the time dependence on the right-hand side is no longer a simple power law but some more general function of time, say,  $p(t)$ . Let us then approximate the temperature distribution by

$$T(z, t) = p(t) y[z/q(t)] , \quad (2.27)$$

where  $y(x)$  is the similarity solution corresponding to the value  $\alpha_0$  of  $\alpha$  and normalized so that  $y(0) = 1$ , and  $q(t)$  is a function to be determined.

Equation (2.27) obeys the boundary and initial conditions  $T(z, 0) = 0$ ,  $T(\infty, t) = 0$ , and  $T(0, t) = p(t)$  if  $q(0) = 0$ . But it does not have the correct form to be a solution of Eq. (1.4) unless  $p(t)$  is a power of  $t$ . So we cannot determine  $q(t)$  by simply substituting Eq. (2.27) into Eq. (1.4): the differential equation (1.4) is too stringent a condition for the trial function (2.27) to satisfy. We can reduce the information content of the differential equation by integrating it over  $z$  from 0 to  $\infty$ . Then it becomes

$$\frac{d}{dt} \int_0^\infty T dz = [-T_z(0)]^{1/3} . \quad (2.28)$$

If we substitute Eq. (2.27) into Eq. (2.28) we get

$$\frac{d}{dt} (pq) = \frac{[-\dot{y}(0)]^{1/3}}{\int_0^\infty y(x) dx} \left(\frac{p}{q}\right)^{1/3} . \quad (2.29)$$

By integrating Eq. (1.19) over  $x$  from 0 to  $\infty$  (and using one integration by parts) we can show that

$$\frac{-[\dot{y}(0)]^{1/3}}{\int_0^\infty y(x) dx} = \frac{\alpha_0 + 1}{\beta_0} . \quad (2.30)$$

Then Eq. (2.29) can be solved for  $q$  in terms of  $p$ ; the solution that obeys the condition  $q(0) = 0$  is

$$q = \frac{1}{p} \left( \frac{4\alpha_0 + 1}{3\beta_0} \int_0^t p^{2/3} dt \right)^{3/4} . \quad (2.31)$$

In Okamura's experiment it is the flux  $Q(t) = [-T_z(0, t)]^{1/3}$  that is imposed. According to Eq. (2.27),

$$Q(t) = \left(\frac{p}{q}\right)^{1/3} [-\dot{y}(0)]^{1/3} = -E(\alpha_0) \left(\frac{p}{q}\right)^{1/3}, \quad (2.32)$$

where  $E(\alpha_0)$  is the number defined in Eq. (1.41). Thus

$$Q(t) = -E(\alpha_0) p^{2/3} \left(\frac{4\alpha_0 + 1}{3\beta_0} \int_0^t p^{2/3} dt\right)^{-1/4}. \quad (2.33)$$

If we set  $u(t) = \int_0^t p^{2/3} dt$ ,  $\dot{u} = p^{2/3}$ , Eq. (2.33) becomes a solvable first-order differential equation for  $u$ . After some computation we find that

$$T(0, t) = p(t) = \left(\frac{\alpha_0 + 1}{\beta_0}\right)^{1/2} [E(\alpha_0)]^{-2} \left(\int_0^t Q dt\right)^{1/2} Q^{3/2}. \quad (2.34)$$

One way to check the accuracy of this formula is to compare the predictions with known, exact results. For the similarity solution belonging to  $\alpha$ , we have from Eq. (1.15) the exact relation

$$T(0, t) = [E(\alpha)]^{-2} Q^2 t^{1/2}, \quad (2.35)$$

where  $Q = Q_* t^{(\alpha-1)/3\beta}$  and  $Q_*$  is a constant of proportionality. If we insert this  $Q$  into Eq. (2.34), we find after some calculation that

$$\frac{T_{\text{approx}}(0, t)}{T_{\text{exact}}(0, t)} = \frac{[(\alpha_0 + 1)/\beta_0]^{1/2} [E(\alpha_0)]^{-2}}{[(\alpha + 1)/\beta]^{1/2} [E(\alpha)]^{-2}}. \quad (2.36)$$

If  $\alpha = 4$ , then  $\beta = 4$ , and  $\alpha/\beta = 1$ . If  $\alpha_0 = 10$ , then  $\beta_0 = 8$ , and  $\alpha_0/\beta_0 = 5/4$ . From Table 1.1 we find  $E(\alpha) = -1.218874$  and  $E(\alpha_0) = -1.270011$  so that the ratio in Eq. (2.36) is 0.966049. Table 2.2 shows some additional results of the same kind.

Table 2.2. Values of  $T_{\text{approx}}(0, t)/T_{\text{exact}}(0, t)$  from Eq. (2.36)

Base case  $\alpha = 4$ ,  $\beta = 4$

$\alpha_0$	$\beta_0$	$\alpha_0/\beta_0$	$T_{\text{approx}}(0, t)/T_{\text{exact}}(0, t)$
10	8	5/4	0.966049
4	4	1	1.000000
2	8/3	3/4	1.044939
1	2	1/2	1.106640
0	4/3	0	1.328809

As expected, the greater the resemblance of the trial  $y$  to the actual  $y$ , the better the approximation.

Okamura et al.<sup>6</sup> imposed a flux  $Q = Q_*[1 + \sin(2\pi\nu t)]$  using various frequencies in their experiments. According to formula (2.34),  $T(0, t)$  vanishes whenever  $Q$  does, so that it should have  $1/\nu$  nodes per unit time, and the envelope of the maxima should vary as  $t^{1/2}$ . Okamura's reported curves of  $T(0, t)$  show the expected sinusoidal modulation, and the envelope of the maximum appears to increase roughly as  $t^{1/2}$ . But the peaks and valleys are not as great as expected from Eq. (2.34), and the valleys never reach zero. However, Okamura's experiment does not conform with the conditions governing formula (2.34). The formula is based on the assumption that the heater has no thermal inertia, whereas Okamura et al. interposed a rather long copper bar between the heater and the He-II bath. Interpreting their results in light of Eq. (2.34) seems to indicate that the heat flux out of the distal end of the copper bar into the helium resembled  $Q = Q_*[1 + k \sin(2\pi\nu t)]$ , where  $k$  is substantially less than 1, rather than the flux  $Q = Q_*[1 + \sin(2\pi\nu t)]$  supplied by the heater to the proximal end of the copper rod.

The final application of Eq. (2.34) is to the following problem: If  $Q = Q_*e^{-t/\tau}$ , under what conditions will the temperature of the front surface never exceed the transition (lambda) temperature? If  $\tau$  is not too small, we might expect the choice  $\alpha_0 = 1$  (clamped-flux solution) to yield a good approximation to the temperature distribution. Then

$$T(0, t) = [Q_*/E(1)]^2 \tau^{1/2} e^{-3t/2\tau} (1 - e^{-t/\tau})^{1/2}. \quad (2.37)$$

The maximum of  $T(0, t)$  occurs when  $e^{-t/\tau} = 3/4$ :

$$T_{\max}(0, t) = \frac{3\sqrt{3}}{16 [E(1)]^2} Q_*^2 \tau^{1/2} = 0.270462 Q_*^2 \tau^{1/2}. \quad (2.38a)$$

Equation (2.38a) is written in special units; in ordinary units it is

$$T_{\max}(0, t) = 0.270462 Q_*^2 (\tau/K^3 S)^{1/2}. \quad (2.38b)$$

Here we must remember that  $T$  represents the temperature rise, so  $T_{\max} = T_\lambda - T_b$  in the problem as stated. As long as  $Q_*\tau^{1/4}$  is less than the value given by Eq. (2.38b), the temperature at the front face will never reach the transition temperature. When  $T_b = 1.8$  K,  $Q_*\tau^{1/4} = 5.37 \text{ W}\cdot\text{cm}^{-2}\cdot\text{s}^{1/4}$ .

**The Clamped-Temperature Problem When  $K$  and  $S$  Vary with Temperature.** All of the work so far has been restricted by the assumption that the properties  $K$  and  $S$  are constant. As it happens, the clamped-temperature problem can be solved in the temperature range from 1.90 to 2.15 K even when  $K$  and  $S$  have their real temperature variations. By comparing this solution with the constant-properties solution, we can determine how accurate the constant-properties solution is. We begin with Eq. (1.2) written for plane geometry,

$$S \frac{\partial T}{\partial t} = \frac{\partial}{\partial z} \left[ K \left( \frac{\partial T}{\partial z} \right)^{1/3} \right]. \quad (2.39)$$

Here  $T$  represents the absolute temperature, *not* the temperature rise. Now we introduce the new variable

$$H = \int_T^{T_\lambda} K^3 dT. \quad (2.40)$$

In terms of  $H$ , Eq. (2.39) becomes

$$\frac{\partial H}{\partial t} = \frac{K^3}{S} \cdot \frac{\partial}{\partial z} \left( \frac{\partial H}{\partial z} \right)^{1/3}. \quad (2.41)$$

Figure 2.7 shows the ratio  $K^3/S$  plotted vs  $H$ ; also shown is the line  $K^3/S = cH^{2/3}$ ,  $c = 73 \text{ cm}^{4/3} \cdot \text{s}^{-1}$ . The error in the fitted line is less than 30% for  $1.9 \text{ K} < T < 2.15 \text{ K}$ , in which range  $K^3/S$  varies by three orders of magnitude. Henceforth, we work in special units in which  $c = 1$ , reconstituting our answer at the end to be valid in any units.

The boundary conditions for the clamped-temperature problem are

$$T(0, t) = T_0 \quad \text{or} \quad H(0, t) = H_0 \equiv H(T_0), \quad (2.42a)$$

$$T(\infty, t) = T_b \quad \text{or} \quad H(\infty, t) = H_b \equiv H(T_b), \quad (2.42b)$$

$$T(z, 0) = T_b \quad \text{or} \quad H(z, 0) = H_b. \quad (2.42c)$$

When  $K^3/S = H^{2/3}$ , Eq. (2.41) is invariant to the family of groups

$$H' = \lambda^\alpha H \quad (2.43a)$$

$$t' = \lambda^{4/3} t \quad (2.43b)$$

$$z' = \lambda z \quad (2.43c)$$

$$0 < \lambda < \infty.$$

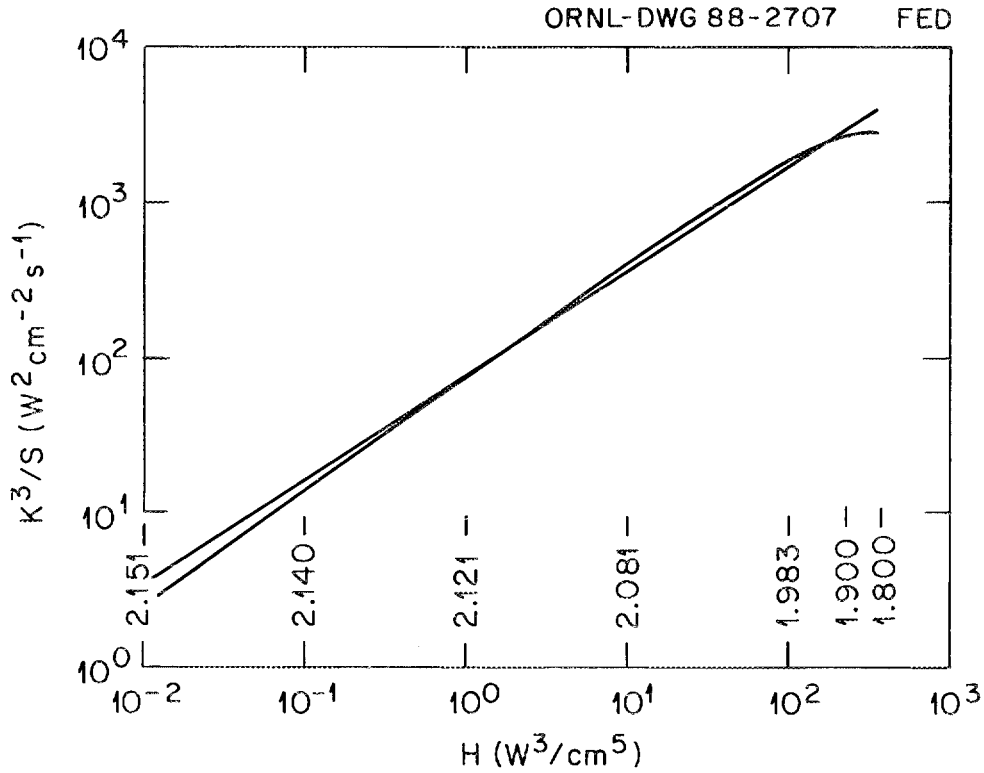


Fig. 2.7. The ratio  $K^3/S$  plotted vs  $H$ . Also shown is the line  $K^3/S = CH^{2/3}$ ,  $C = 73 \text{ cm}^{4/3} \cdot \text{s}^{-1}$ .

The similarity solutions that obey the boundary and initial conditions (2.42) belong to the value  $\alpha = 0$  of the parameter  $\alpha$  and accordingly take the form

$$H = y \left( z/t^{3/4} \right). \quad (2.44)$$

The coefficients in the constraint equation (1.6) are  $M = 0$ ,  $N = 3$ ,  $L = 4$ . To see what the group (1.8) becomes in this case, it is best first to substitute  $\nu = \mu^{L/M}$  and write it as

$$y' = \nu y \quad \left. \vphantom{y' = \nu y} \right\} \quad (2.45a)$$

$$x' = \nu^{M/L} x \quad \left. \vphantom{x' = \nu^{M/L} x} \right\} \quad 0 < \nu < \infty, \quad (2.45b)$$

which becomes

$$y' = \nu y \quad \left. \vphantom{y' = \nu y} \right\} \quad (2.46a)$$

$$x' = x \quad \left. \vphantom{x' = x} \right\} \quad 0 < \nu < \infty \quad (2.46b)$$

when  $M = 0$ ,  $N = 3$ , and  $L = 4$ .

If we substitute Eq. (2.44) into Eq. (2.41) with  $K^3/S = H^{2/3}$ , we get

$$y^{2/3} \frac{d}{dx} \left( \dot{y}^{1/3} \right) + \frac{3}{4} x \dot{y} = 0, \quad (2.47)$$

which is, as expected, invariant to the group (2.46). The three boundary conditions (2.42) now collapse to the two conditions

$$y(0) = H_0, \quad (2.48a)$$

$$y(\infty) = H_b. \quad (2.48b)$$

The heat flux through the front surface is given by

$$q = -K \left( \frac{\partial T}{\partial z} \right)_{z=0}^{1/3} = \left( \frac{\partial H}{\partial z} \right)_{z=0}^{1/3} = [\dot{y}(0)]^{1/3} t^{-1/4}, \quad (2.49a)$$

which can be written

$$qt^{1/4} = [\dot{y}(0)]^{1/3} = \left[ \frac{\dot{y}(0)}{y(\infty)} \right]^{1/3} H_b^{1/3}. \quad (2.49b)$$

Now the three quantities  $\dot{y}(0)$ ,  $y(0) = H_0$ , and  $y(\infty) = H_b$  are functionally related, for if we know  $y(0)$  and  $\dot{y}(0)$  we can calculate  $y(\infty)$  by integrating Eq. (2.47). The functional relation must be invariant to Eq. (2.46) (augmented by the additional obvious requirement that  $\dot{y}' = \nu \dot{y}$ ). The only possibility is

$$\frac{\dot{y}(0)}{y(\infty)} = F \left[ \frac{y(\infty)}{y(0)} \right] = F \left( \frac{H_b}{H_0} \right). \quad (2.50)$$

Then, Eq. (2.49b) becomes, in ordinary units,

$$qt^{1/4} = \left[ F \left( \frac{H_b}{H_0} \right) \right]^{1/3} c^{-1/4} H_b^{1/3} \quad (\text{ordinary units}). \quad (2.51)$$

This needs to be compared with the constant-properties result [cf. Eqs. (1.24a) and (1.25)]

$$qt^{1/4} = \left( \sqrt{3}/2 \right)^{1/2} (K^3 S)^{1/4} (T_0 - T_b)^{1/2}. \quad (2.52)$$

To make this comparison, we need to do two things. First, we need to calculate the function  $F$ . This we can do by repeated integration of Eq. (2.47) using the initial value  $y(0) = 1$  and various  $\dot{y}(0)$ . Second, we need to determine what constant values of  $K$  and  $S$  to substitute into Eq. (2.52) in order to compare it with Eq. (2.51). If  $K^3/S$  were truly equal to  $cH^{2/3}$ , then Eq. (2.51) would be exact. The relation between  $H$  and  $T$  is determined by whatever functional dependence we take for  $K$  on  $T$ , so we must choose  $K_b$  in accordance with it. The value of  $S_b$  that corresponds

to the “exact” law  $K^3/S = cH^{2/3}$  is then  $S_b = K_b^3/cH_b^{2/3}$ . When these values are substituted into Eq. (2.52) we get a comparison of it with Eq. (2.51) that does not depend on the goodness of the fit of  $cH^{2/3}$  to the real  $K^3/S$ .

The function  $K(T)$  used in computing  $H(T)$  is a correlation recommended by van Sciver<sup>12</sup>; it is shown in Fig. 2.8. Shown also is van Sciver’s recommended correlation for  $S(T)$ . Shown in Fig. 2.9 is the fractional difference between the left-hand sides of Eqs. (2.52) and (2.51) for  $T_b = 1.9$  K as a function of  $T_0$ . The fractional difference is small (<5%) until  $T_0$  approaches  $T_\lambda$ , where  $K$  has a precipitous fall towards zero. When  $T_0 = T_\lambda$ , the fractional difference has its largest value, namely, 20%. The real value of  $S_b$  obtained from Fig. 2.8 is about 4% higher than the value  $K_b^3/cH_b^{2/3}$ . Since the right-hand side of Eq. (2.52) depends on  $S^{1/4}$ , using the real value of  $S_b$  will only change the results in Fig. 2.9 by roughly +0.01. So for  $T_b = 1.9$  K, at least, the constant-properties solution gives the flux through the front face correct to within 20% or better. This comparatively small error in the constant-properties flux in the face of a rather strong dependence of  $K$  on  $T$  accounts for the good agreement with experiment of the theory of stabilization of superconductors presented earlier.

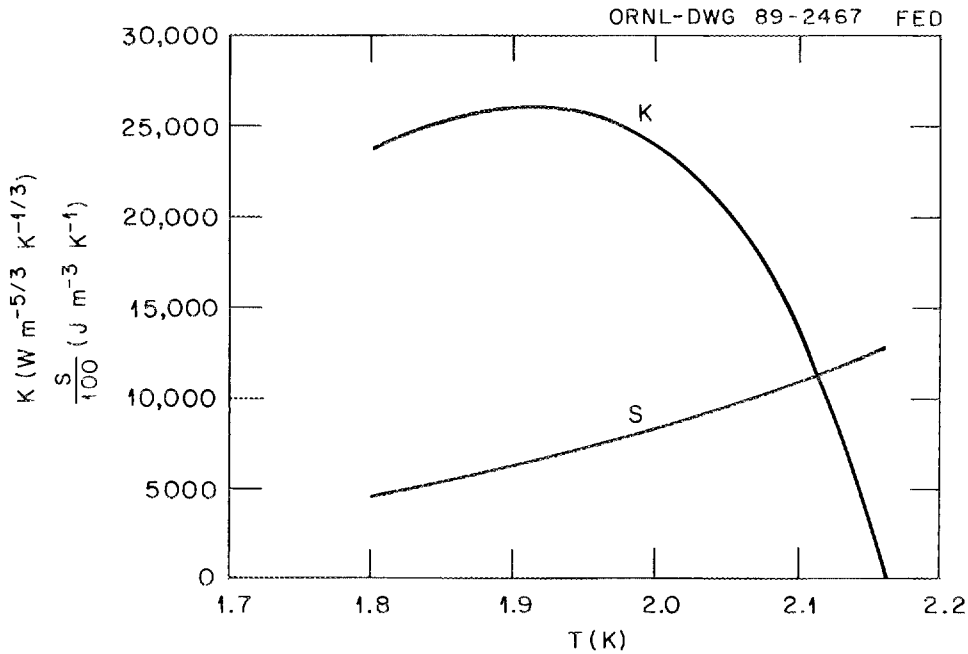


Fig. 2.8. Correlations made by van Sciver<sup>12</sup> for the superfluid heat conductivity  $K$  and the volumetric heat capacity  $S$  as functions of temperature  $T$ .

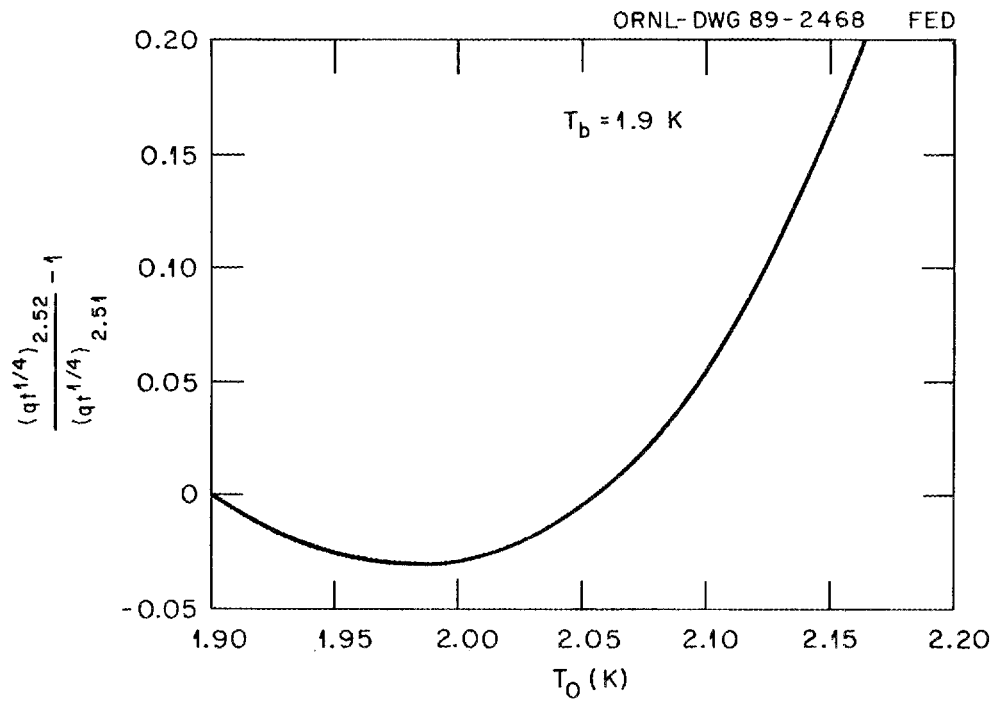


Fig. 2.9. The fractional difference between the constant-properties value of  $qt^{1/4}$  [Eq. (2.52)] and the real-properties value of  $qt^{1/4}$  [Eq. (2.51)] as a function of the temperature  $T_0$  of the heated surface.



**CHAPTER 3**  
**TIME-INDEPENDENT PROBLEMS; COMPLEMENTARY**  
**VARIATIONAL PRINCIPLES**

**Introduction.** We begin with the problem of the steady flow of heat through an irregular, He-II-filled duct. The lateral surface of the duct is impervious to heat; the end surfaces are isotherms. The problem is to calculate the steady flow of heat  $Q$  through the duct as a function of its shape and the temperatures  $T_1$  and  $T_2$  of its isothermal surfaces.

The equation that governs the steady temperature distribution in the duct is the time-independent version of Eq. (1.2), namely,

$$\nabla \cdot [K (\nabla T)^{1/3}] = 0 . \quad (3.1a)$$

Under the assumption of *constant properties* ( $K$  independent of  $T$ ), which *applies throughout this chapter*, Eq. (3.1a) becomes

$$\nabla \cdot (\nabla T)^{1/3} = 0 . \quad (3.1b)$$

The attack is by means of complementary variational principles.<sup>13,14</sup> Complementary variational principles are a pair of functionals one of which attains a minimum and the other an equal maximum for exact solutions of a related differential equation. Trial functions therefore provide two estimates of the quantity represented by the functional one of which is an upper limit, the other of which is a lower limit, and both of which are accurate to second order in the error in the trial function.

Reference 14 gives a thorough description of how to construct a pair of variational principles; therefore, I shall simply state the variational principles for Eq. (3.1b). But I shall prove here that they have the properties ascribed to them. Let

$$A_+ = \int_V |\nabla T|^{4/3} dV \quad (3.2)$$

and

$$A_- = -\frac{1}{3K^4} \int_V q^4 dV - \frac{4}{3K} \int_S T_* \vec{q} \cdot \vec{dS} , \quad (3.3)$$

where  $V$  is the interior volume of the duct,  $S$  is its total surface,  $T_*$  is the exact solution of Eq. (3.1b) corresponding to the isothermal-adiabatic boundary conditions mentioned above,  $T$  is a trial function obeying the boundary conditions  $T = T_2$  and

$T = T_1$  on the isothermal surfaces, and  $\vec{q}$  is a divergenceless trial vector. Then, as we shall show below,

$$A_+ \geq A_* = Q(T_2 - T_1)/K \geq A_- , \quad (3.4)$$

with equality holding when  $T = T_*$  and  $\vec{q} = \vec{q}_* = -K(\nabla T_*)^{1/3}$ .

The appearance of  $Q$  in the value of  $A_*$  is the reason for the usefulness of the complementary functionals  $A_+$  and  $A_-$ , for they provide upper and lower bounds to the quantity we are seeking, accurate to *second order* in the error in our trial functions.

Suppose the trial function  $T$  in Eq. (3.2) is written as  $T = T_* + \epsilon$ , where  $T_*$  is the exact temperature distribution and  $\epsilon$  is the small difference of  $T$  from  $T_*$ . To terms of second order in  $\epsilon$ , the integrand in Eq. (3.2) is

$$|\nabla T|^{4/3} = |\nabla T_*|^{4/3} + \frac{4}{3} \frac{\nabla T_* \cdot \nabla \epsilon}{|\nabla T_*|^{2/3}} + \frac{2}{3} \frac{(\nabla \epsilon)^2}{|\nabla T_*|^{2/3}} - \frac{4}{9} \frac{(\nabla T_* \cdot \nabla \epsilon)^2}{|\nabla T_*|^{8/3}} + \dots \quad (3.5)$$

We denote the integral over  $V$  of the first term by  $A_*$  [which we have yet to show equals  $Q(T_2 - T_1)/K$ ]. The integral over  $V$  of the second term is zero:

$$\int_V \frac{\nabla T_* \cdot \nabla \epsilon}{|\nabla T_*|^{2/3}} dV = \int_V (\nabla T_*)^{1/3} \cdot \nabla \epsilon dV = \int_V \nabla \cdot [\epsilon (\nabla T_*)^{1/3}] dV = \int_S \epsilon (\nabla T_*)^{1/3} \cdot d\vec{S} . \quad (3.6)$$

The first equality follows from the definition of  $(\nabla T_*)^{1/3}$ , the second from the fact that  $T_*$  satisfies Eq. (3.1b), and the third from the divergence theorem. The last integral vanishes because on the isothermal surfaces  $\epsilon = 0$  (since  $T = T_*$  there), whereas on the adiabatic surfaces  $(\nabla T_*)^{1/3} \cdot d\vec{S} = 0$  [see Eq. (1.1)]. The sum of the two second-order terms in Eq. (3.5) is always positive, as we can see by noting that  $(\nabla T_* \cdot \nabla \epsilon)^2 \leq (\nabla T_*)^2 (\nabla \epsilon)^2$ . Thus  $A_+$  differs from  $A_*$  by a positive term of second order in  $\epsilon$ .

To evaluate  $A_*$  we proceed as follows:

$$\begin{aligned} A_* &= \int_V |\nabla T_*|^{4/3} dV = \int_V (\nabla T_*)^{1/3} \cdot (\nabla T_*) dV \\ &= -\frac{1}{K} \int_V \vec{q}_* \cdot \nabla T_* dV \\ &= -\frac{1}{K} \int_V \nabla \cdot (\vec{q}_* T_*) dV \quad (\text{since } \nabla \cdot \vec{q}_* = 0) \\ &= -\frac{1}{K} \int_S T_* \vec{q}_* \cdot d\vec{S} . \end{aligned} \quad (3.7)$$

On the adiabatic surfaces  $\vec{q}_* \cdot d\vec{S} = 0$ . On the high-temperature isothermal surface  $T_* = T_2$  and  $-\int_S \vec{q}_* \cdot d\vec{S} = Q$ . On the low-temperature isothermal surface  $T_* = T_1$  and  $\int_S \vec{q}_* \cdot d\vec{S} = Q$ . Thus the last line of Eq. (3.7) becomes

$$A_* = Q(T_2 - T_1)/K. \quad (3.8)$$

We treat  $A_-$  in a similar way. Suppose we set  $\vec{q} = \vec{q}_* + \vec{\epsilon}$ , where  $\nabla \cdot \vec{\epsilon} = 0$  so that  $\vec{q}$  is divergenceless, as required. Then, to terms of second order in  $\vec{\epsilon}$ ,

$$\begin{aligned} A_- = & -\frac{1}{3K^4} \int_V q_*^4 dV - \frac{4}{3K^4} \int_V q_*^2 \vec{q}_* \cdot \vec{\epsilon} dV - \frac{1}{3K^4} \int_V [2q_*^2 \epsilon^2 + 4(q_* \cdot \epsilon)^2] dV \\ & - \frac{4}{3K} \int_S T_* \vec{q}_* \cdot d\vec{S} - \frac{4}{3K} \int_S T_* \vec{\epsilon} \cdot d\vec{S}. \end{aligned} \quad (3.9)$$

Remembering that  $\vec{q}_* = -K(\nabla T_*)^{1/3}$  and using Eq. (3.7), we can show that the sum of the first and fourth terms on the right-hand side of Eq. (3.9) is  $A_*$ . Remembering also that  $\nabla \cdot \vec{\epsilon} = 0$  and using the divergence theorem, we can further show that the sum of the second and fifth terms vanishes. The integrand in the third term being positive, we then see that  $A_-$  differs from  $A_*$  by a negative term of second order in  $\vec{\epsilon}$ .

**Comparison of the Superfluid and the Ordinary Conductance.** The quantity

$$\Gamma = \frac{Q}{V^{2/3} K [(T_2 - T_1)/V^{1/3}]^{1/3}} \quad (3.10a)$$

is a dimensionless measure of the total heat flow  $Q$  through the duct. I call it the superfluid conductance of the duct. If the duct were filled with an ordinary conductive material that obeyed Fourier's law  $\vec{q} = -k\nabla T$ , its conductance would be

$$\Gamma_0 = \frac{Q_0}{V^{2/3} k [(T_2 - T_1)/V^{1/3}]} \quad (3.10b)$$

where  $Q_0$  is the total heat flow through the duct in the case of ordinary conduction. These conductances are related, as we now show using the functional  $A_+$ .

According to Eqs. (3.2) and (3.4)

$$Q(T_2 - T_1)/K \leq \int_V (\nabla T)^{4/3} dV, \quad (3.11)$$

where  $T$  is a trial function assuming the values  $T_2$  and  $T_1$  on the isothermal duct surfaces. Now theorem 192 of Hardy, Littlewood, and Polya<sup>15</sup> says that

$$\left[ \frac{1}{V} \int_V (\nabla T)^{4/3} dV \right]^{3/4} \leq \left[ \frac{1}{V} \int_V (\nabla T)^2 dV \right]^{1/2} \quad (3.12)$$

so that

$$\frac{Q(T_2 - T_1)}{KV^{1/3}} \leq \left[ \int_V (\nabla T)^2 dV \right]^{2/3}. \quad (3.13)$$

Now we choose the trial function  $T$  to be the exact temperature distribution in the case of ordinary conduction. It is then easy to show that the right-hand side of Eq. (3.13) is  $Q_0(T_2 - T_1)/k$ . Thus

$$\Gamma = \frac{Q}{V^{2/3}K[(T_2 - T_1)/V^{1/3}]^{1/3}} \leq \left\{ \frac{Q_0}{V^{2/3}k[(T_2 - T_1)/V^{1/3}]} \right\}^{2/3} = \Gamma_0^{2/3}, \quad (3.14)$$

which says that the superfluid conductance of a duct is bounded from above by the two-thirds power of the ordinary conductance of the duct. The usefulness of this result comes from the fact that the ordinary conductance can be measured easily at room temperature using an electrical analog or can be calculated for a variety of complex shapes by conformal mapping.

In a duct shaped like a rectangular parallelepiped,  $|\nabla T| = (T_2 - T_1)/L$ , where  $L$  is the distance between the two parallel isothermal surfaces, irrespective of whether the heat is transferred by ordinary or by superfluid conduction. Then, the left- and right-hand sides of Eq. (3.11) are equal to each other, as are those of Eq. (3.12). So for a parallelepipedal duct, the left- and right-hand sides of Eq. (3.14) are equal.

It is comparatively simple to calculate the ordinary and superfluid conductances of a duct in the form of a prism of unit height whose base is a sector of a cylindrical annulus. The inner and outer radii of the annulus are  $R_2$  and  $R_1$ , respectively. The isothermal surfaces are  $r = R_2$  and  $r = R_1$ . Then a short computation shows that

$$\frac{\Gamma}{\Gamma_0^{2/3}} = \left( \frac{2\rho \ln \rho}{\rho^2 - 1} \right)^{2/3}; \quad \rho = R_1/R_2. \quad (3.15)$$

The corresponding result for a sector of a spherical annulus is

$$\frac{\Gamma}{\Gamma_0^{2/3}} = \left[ \frac{15\rho^3(\rho - 1)^2}{(\rho^5 - 1)(\rho^3 - 1)} \right]^{1/3}; \quad \rho = R_1/R_2. \quad (3.16)$$

Figure 3.1 shows both of these ratios plotted against the ratio  $\rho$  of the outer and inner radii. These curves, when properly interpreted, show that except in the

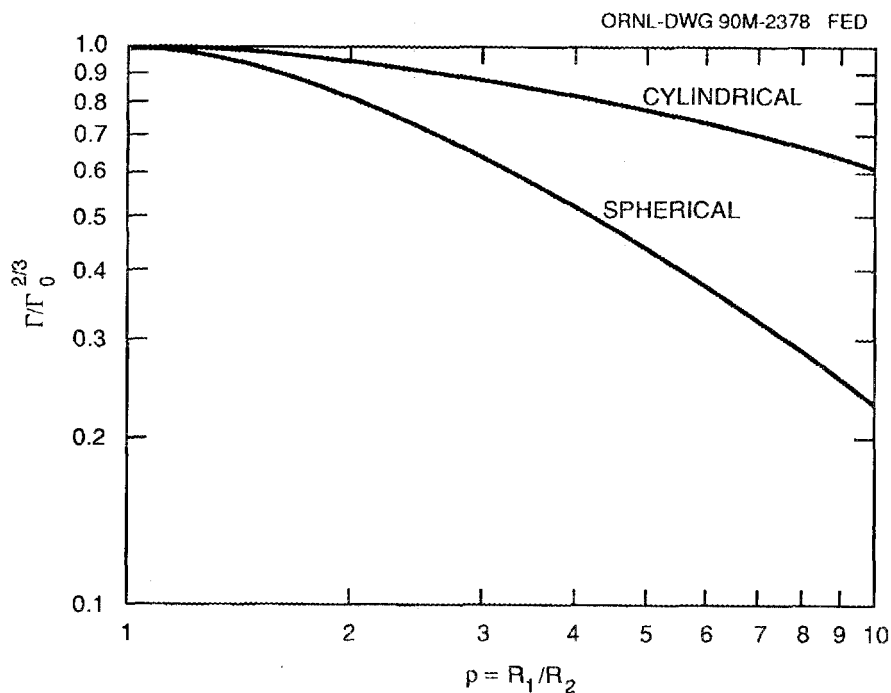


Fig. 3.1. The ratio of the superfluid conductance to the two-thirds power of the ordinary conductance for cylindrical and spherical annular ducts. The abscissa is the ratio of the inner and outer duct radii.

most extreme cases the two sides of Eq. (3.14) should be fairly close to one another. Consider, for example, the case of  $\rho = 3$ . In the cylindrical annulus, the temperature gradient changes by a factor of 3 for normal conduction and by a factor of 27 for superfluid conduction. Yet  $\Gamma/\Gamma_0^{2/3} = 0.879$ . In the spherical annulus, the situation is even more extreme, with the temperature gradient changing by the respective factors 9 and 729. Yet  $\Gamma/\Gamma_0^{2/3} = 0.636$ . Hence the condition of constant temperature gradient, which makes  $\Gamma/\Gamma_0^{2/3} = 1$ , can be quite severely violated without  $\Gamma/\Gamma_0^{2/3}$  departing substantially from 1.

**The Two-Dimensional, Irregularly Shaped Duct.** The duct occupies the region  $R$  bounded by two parallel planes a distance  $L$  apart, each of which is an isotherm. The adiabatic sides of the duct are the curves  $y = Y_1(x)$  and  $y = Y_2(x)$ , with  $Y_1 > Y_2$  (see Fig. 3.2). Suppose we choose our trial function  $T$  in  $A_+$  to be a function of  $x$  only, that is,  $T = T(x)$ . To satisfy the boundary conditions on the isothermal surfaces we must have  $T(0) = T_2$  and  $T(L) = T_1$ . Then

$$A_+ = \int_0^L \left( \frac{dT}{dx} \right)^{4/3} (Y_1 - Y_2) dx . \quad (3.17)$$

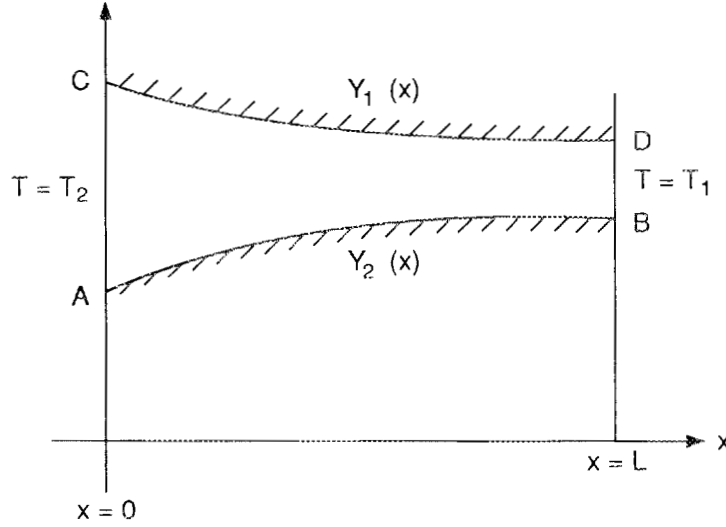


Fig. 3.2. The He-II-filled duct with isothermal surfaces  $x = 0$  and  $x = L$  and adiabatic surfaces  $y = Y_1(x)$  and  $y = Y_2(x)$ .

We choose the dependence of  $T$  on  $x$  to make  $A_+$  a minimum; that is, we choose  $T$  so that

$$\delta A_+ = \int_0^L \frac{4}{3} \left( \frac{dT}{dx} \right)^{1/3} \delta \left( \frac{dT}{dx} \right) (Y_1 - Y_2) dx = 0. \quad (3.18)$$

Since  $\delta$  and  $\frac{d}{dx}$  commute, we can integrate by parts in Eq. (3.18) and get

$$\frac{4}{3} \int_0^L \frac{d}{dx} \left[ \left( \frac{dT}{dx} \right)^{1/3} (Y_1 - Y_2) \right] \delta T dx = 0. \quad (3.19)$$

The integrated term in Eq. (3.19) vanishes because  $\delta T = 0$  at  $x = 0$  and  $x = L$ ; this is because the trial function  $T$  must obey the boundary conditions  $T(0) = T_2$ ,  $T(L) = T_1$ . Thus  $T$  satisfies the Euler-Lagrange equation

$$\frac{d}{dx} \left[ \left( \frac{dT}{dx} \right)^{1/3} (Y_1 - Y_2) \right] = 0 \quad (3.20)$$

so that

$$\left( \frac{dT}{dx} \right)^{1/3} = \frac{-B}{Y_1 - Y_2}, \quad (3.21)$$

where  $B$  is a constant of integration determined by

$$T_2 - T_1 = B^3 \int_0^L \frac{dx}{(Y_1 - Y_2)^3} \quad (3.22)$$

If we substitute Eqs. (3.21) and (3.22) into Eq. (3.17), we find after some rearrangement that

$$A_+ = (T_2 - T_1)^{4/3} \left[ \int_0^L (Y_1 - Y_2)^{-3} dx \right]^{-1/3}. \quad (3.23)$$

Then since  $A_+ \geq A_*$ , we have, using Eq. (3.8),

$$\frac{Q}{K(T_2 - T_1)^{1/3}} \leq \left[ \int_0^L (Y_1 - Y_2)^{-3} dx \right]^{-1/3}. \quad (3.24)$$

**The Two-Dimensional, Irregularly Shaped Duct** (continued). Now we turn to the evaluation of  $A_-$  given in Eq. (3.3). Since  $\vec{q}$  must be a divergenceless vector, we introduce a stream function  $\psi$  and set

$$q_x = \frac{\partial \psi}{\partial y}, \quad q_y = -\frac{\partial \psi}{\partial x}. \quad (3.25)$$

To evaluate the surface integral in Eq. (3.3) we need to know  $T_*$  on  $S$ , the bounding surface of the duct. We know it only on the isotherms, not on the lateral, adiabatic surfaces, that is, not on  $y = Y_1$  and  $y = Y_2$ . But if we take  $y = Y_1$  and  $y = Y_2$  to be level surfaces of  $\psi$ ,  $\vec{q} \cdot d\vec{S}$  will be zero on them. Then

$$-\frac{4}{3K} \int_S T_* \vec{q} \cdot d\vec{S} = \frac{4}{3K} (T_2 - T_1) \int_{Y_2}^{Y_1} \frac{\partial \psi}{\partial y} dy = \frac{4}{3K} (T_2 - T_1) (\psi_1 - \psi_2). \quad (3.26)$$

Now in order that our trial functions may include the exact solution, we take

$$\psi_1 - \psi_2 = \int_{Y_2}^{Y_1} \frac{\partial \psi}{\partial y} dy = \int_{Y_2}^{Y_1} q_{*x} dy = Q. \quad (3.27)$$

Combining Eqs. (3.26), (3.27), (3.3), and (3.4), we find

$$\frac{Q(T_2 - T_1)}{K} \leq \frac{1}{K^4} \int_V (\nabla \psi)^4 dV. \quad (3.28)$$

In spite of the direction of this inequality, it will ultimately provide a lower limit to  $Q$  because  $\psi$  also involves  $Q$ .

We choose as level surfaces for the trial function  $\psi$  the surfaces

$$y = \lambda Y_1(x) + (1 - \lambda) Y_2(x), \quad 0 \leq \lambda \leq 1. \quad (3.29)$$

This procedure is called by Polya and Szegö<sup>16</sup> the method of assigned level surfaces.

The most convenient way to evaluate the integral in Eq. (3.28) is to introduce the new coordinates  $\lambda, x$ . Since the new coordinates are not Cartesian, we employ

tensor formalism for the calculations. In terms of  $x$  and  $\lambda$ , the squared distance between two neighboring points is given by

$$(dx)^2 + (dy)^2 = (dx)^2 + \{ (Y_1 - Y_2)d\lambda + [\lambda\dot{Y}_1 + (1 - \lambda)\dot{Y}_2]dx \}^2 . \quad (3.30)$$

The components of the metric tensor are then

$$\begin{aligned} g_{xx} &= 1 + [\lambda\dot{Y}_1 + (1 - \lambda)\dot{Y}_2]^2 , \\ g_{x\lambda} &= g_{\lambda x} = [\lambda\dot{Y}_1 + (1 - \lambda)\dot{Y}_2](Y_1 - Y_2) , \\ g_{\lambda\lambda} &= (Y_1 - Y_2)^2 , \\ g &= \det(g_{ij}) = (Y_1 - Y_2)^2 , \\ g^{\lambda\lambda} &= \frac{g_{xx}}{g} = \frac{1 + [\lambda\dot{Y}_1 + (1 - \lambda)\dot{Y}_2]^2}{(Y_1 - Y_2)^2} . \end{aligned} \quad (3.31)$$

If  $\psi$  is a function only of  $\lambda$ ,

$$(\nabla\psi)^4 = \left[ g^{\lambda\lambda} \left( \frac{d\psi}{d\lambda} \right)^2 \right]^2 . \quad (3.32)$$

Since

$$\iint_R (\nabla\psi)^4 dx dy = \iint_R (\nabla\psi)^4 \sqrt{g} d\lambda dx , \quad (3.33)$$

we finally have

$$\iint_R (\nabla\psi)^4 dx dy = \int_0^1 d\lambda \left( \frac{d\psi}{d\lambda} \right)^4 \int_0^L dx \frac{\{1 + [\lambda\dot{Y}_1 + (1 - \lambda)\dot{Y}_2]^2\}^2}{(Y_1 - Y_2)^3} . \quad (3.34)$$

The right-hand side of Eq. (3.34) has the form

$$\int_0^1 d\lambda \left( \frac{d\psi}{d\lambda} \right)^4 G(\lambda) , \quad (3.35)$$

where  $G(\lambda)$  is  $\int_0^L \dots dx$ . We choose  $\psi$  so as to minimize Eq. (3.35). A short variational calculation shows that  $\psi$  must obey the Euler-Lagrange differential equation

$$\frac{d}{d\lambda} \left[ G(\lambda) \left( \frac{d\psi}{d\lambda} \right)^3 \right] = 0 . \quad (3.36)$$

The solution that obeys the boundary conditions  $\psi_1 = Q$ ,  $\psi_2 = 0$  [see Eq. (3.27)] is

$$\psi = Q \frac{\int_0^\lambda G^{-1/3} d\lambda}{\int_0^1 G^{-1/3} d\lambda} . \quad (3.37)$$

Substituting Eq. (3.37) into Eq. (3.35), we find that Eq. (3.28) takes the form

$$\frac{Q(T_2 - T_1)}{K} \leq \left(\frac{Q}{\bar{K}}\right)^4 \left(\int_0^1 G^{-1/3} d\lambda\right)^{-3} \quad (3.38a)$$

or

$$\frac{Q}{K(T_2 - T_1)^{1/3}} \geq \int_0^1 G^{-1/3} d\lambda, \quad (3.38b)$$

where

$$G(\lambda) = \int_0^L \frac{\{1 + [\lambda \dot{Y}_1 + (1 - \lambda) \dot{Y}_2]^2\}^2}{(Y_1 - Y_2)^3} dx. \quad (3.38c)$$

The function  $G$  is simple to evaluate when the adiabatic surfaces are straight lines, that is, when  $R$  is a trapezoid. By way of example, consider the trapezoid shown in Fig. 3.3, for which  $\dot{Y}_1 = -a$  and  $\dot{Y}_2 = 0$ . In this case, Eq. (3.38b) becomes

$$Q \geq \frac{K(T_2 - T_1)^{1/3}}{[\int_0^L dx / (Y_1 - Y_2)^3]^{1/3}} \cdot \int_0^1 (1 + \lambda^2 a^2)^{-2/3} d\lambda. \quad (3.39)$$

ORNL-DWG 87C-2348 FED

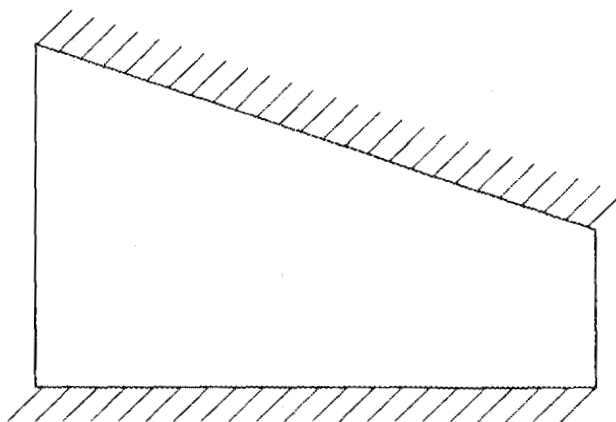


Fig. 3.3. A trapezoidal duct. The hatched surfaces are adiabatic.

Comparing Eq. (3.39) with Eq. (3.24), we see that the  $\lambda$ -integral in Eq. (3.39) gives the ratio of the upper and lower variational estimates of  $Q$ . The  $\lambda$ -integral is easy to evaluate either by series or with Simpson's rule. A few values are given in Table 3.1. These numerical values show that even for substantial slopes the two bracketing estimates are quite close together.

Table 3.1. Values of the integral

$$\int_0^1 (1 + \lambda^2 a^2)^{-2/3} d\lambda$$

$a$	$\int_0^1 (1 + \lambda^2 a^2)^{-2/3} d\lambda$
0.0	1.000000
0.1	0.997789
0.3	0.980852
0.5	0.950452
0.7	0.911607
1.0	0.847138
1.5	0.743754
2.0	0.656516

**Tube Banks.** The variational estimates (3.24) and (3.38b) can be applied to superfluid heat conduction transverse to a bank of tubes. Imagine a pair of parallel planes a distance  $\Delta x$  apart. One plane is maintained at the temperature  $T_2$  and the other at the temperature  $T_1$ . Between the planes lie many tubes of a lattice (square or triangular) of tubes. The lattice pitch (center-to-center spacing)  $2L$  is therefore  $\ll \Delta x$ . We wish to express the heat flux between the planes as a fraction  $f$  of the heat flux  $K[(T_2 - T_1)/\Delta x]^{1/3}$  that would flow in the absence of the tubes. The tubes are considered impervious to heat.

Figure 3.4(a) shows a portion of a square lattice. Owing to the symmetry of the lattice, the horizontal lines shown in the figure are streamlines of the heat flow and the vertical lines are isotherms. The boldly outlined area can be considered a duct of the kind we have just considered. The result of applying Eq. (3.24) to this duct is shown in Fig. 3.5 as the curve of  $f$  vs  $\rho = R/L_S$  marked "square lattice, upper bound." A similarly obtained bound for the triangular lattice is also shown in Fig. 3.5 (ref. 17).

In applying Eq. (3.38b) to the duct in Fig. 3.4(a), the following difficulty is encountered. Because the slope  $\dot{Y}_2$  becomes infinite at  $x = R$ , the lower limit given by Eq. (3.38) is  $f = 0$ . While a correct lower bound, this value is not of much practical use. We can evade this difficulty, *but at the price of variational accuracy*. It can be shown<sup>17</sup> that the value of  $f$  for the effective duct shown in Fig. 3.4(b) is less than that for the duct shown in Fig. 3.4(a). Shown in Fig. 3.5 are lower bounds

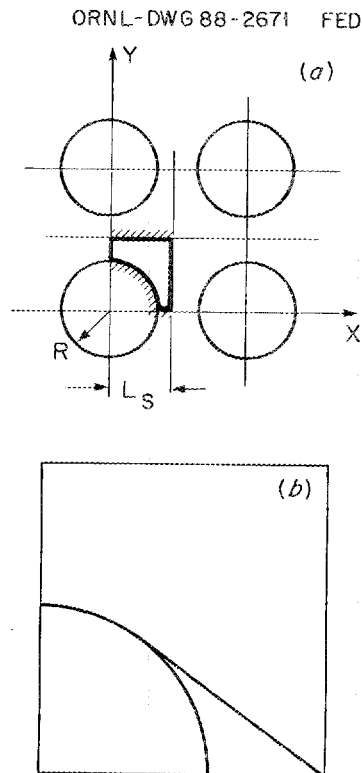


Fig. 3.4. Sketch of (a) the unit duct for the square lattice and (b) the effective duct for calculating a lower bound. The hatched surfaces are adiabatic.

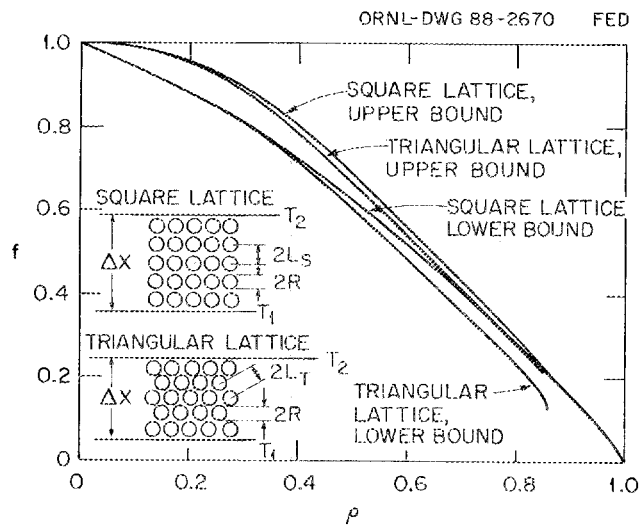


Fig. 3.5. Upper and lower bounds to the correction factor  $f$  for the square triangular lattices as a function of  $\rho$ , the diameter-to-pitch ratio.

to  $f$  based on applying Eq. (3.38b) to this effective duct for both the square and triangular lattices.

The empirical function  $f = (1 - \rho)(1 + 2\rho)/(1 + \rho)$ , where  $\rho$  is the diameter-to-pitch ratio, fits the two upper bounds rather closely ( $<4\%$  for  $\rho < 0.85$ ) and is recommended for design purposes.

As a postscript to this section, I shall add a brief application of this formula to the design of tube-in-shell heat exchangers for He-II. In a tube-in-shell heat exchanger, hot fluid flows through a bank of parallel tubes immersed in a constantly renewed cold bath. In the example we consider here, the hot fluid is pressurized He-I and the cold bath is a pumped bath of saturated He-II. The purpose of the heat exchange is to make pressurized He-II in the tubes. In this way, for example, the helium corresponding to point  $P$  in Fig. 2.1 can be made available for technical purposes.

The effectiveness of the heat exchanger is greatly decreased if the He-II in the bath boils anywhere but at the free surface (see the schematic diagram in Fig. 3.6). As we descend from the free surface, the bath temperature  $T$  increases from the saturation temperature  $T_S(P)$ , where  $P$  is the pressure maintained by the pump. The saturation temperature  $T_S$  also increases with depth because of the pressure

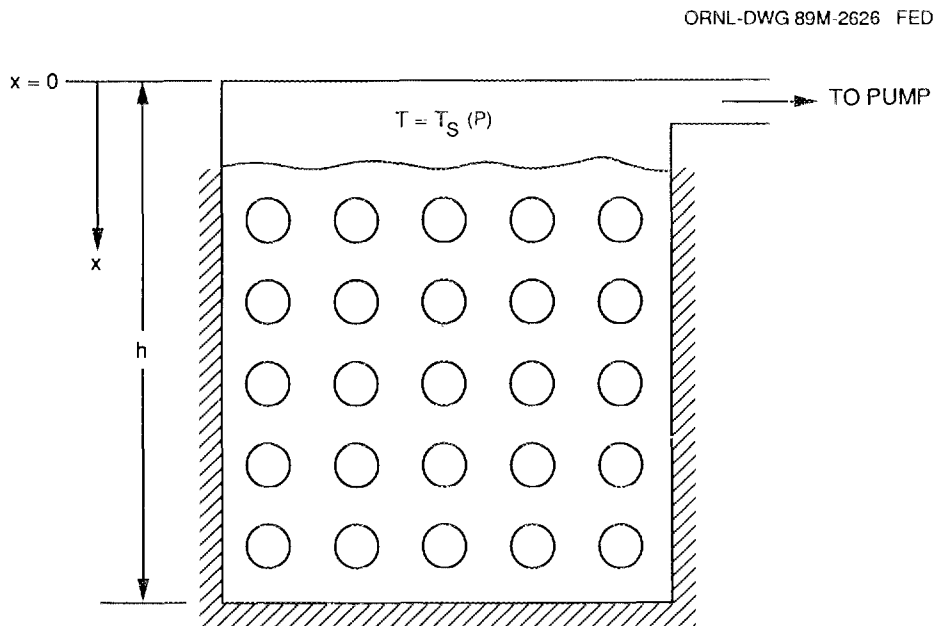


Fig. 3.6. Schematic diagram of a tube-in-shell heat exchanger.

head  $\rho_d g x$  the helium experiences. If  $T < T_S$  everywhere but at  $x = 0$ , no volume boiling will occur.

To calculate  $T$ , we must specify the total thermal power  $Q$  being transferred from the tubes to the bath (units of  $Q$ :  $\text{W}\cdot\text{m}^{-3}$ ). We assume that this power is uniformly deposited in the bath. Treating the bath as a uniform continuum, we then write for its steady temperature the differential equation

$$fK \frac{d}{dx} \left( \frac{dT}{dx} \right)^{1/3} + Q = 0. \quad (3.40)$$

Here the factor  $f$  accounts, as discussed above, for the partial occlusion of the flow space in the bath by the tubes. Equation (3.40) is based on the assumption that  $K$  can be treated as a constant independent of  $T$ . This is an extremely good approximation here because of the small temperature rise that occurs in the bath.

We need to solve Eq. (3.40) subject to the boundary conditions  $T = T_S(P)$  at  $x = 0$  and  $dT/dx = 0$  at  $x = h$  (we treat the hatched surfaces in Fig. 3.6 as adiabatic). The solution we seek is

$$T = T_S(P) + \frac{h^4}{4} \left( \frac{Q}{fK} \right)^3 \left[ 1 - \left( 1 - \frac{x}{h} \right)^4 \right]. \quad (3.41)$$

The saturation temperature at depth  $x$  with which Eq. (3.41) needs to be compared is

$$T_S = T_S(P) + \left( \frac{dT}{dP} \right)_S \rho_d g x. \quad (3.42)$$

Now Eq. (3.41) is concave downwards for  $0 < x < h$  and so will always be less than Eq. (3.42) if the slope of Eq. (3.41) at  $x = 0$  is less than the slope of Eq. (3.42) at  $x = 0$ . Thus the condition of no volume boiling is

$$\left( \frac{Qh}{fK} \right)^3 < \left( \frac{dT}{dP} \right)_S \rho_d g. \quad (3.43)$$

As a typical example let us take  $T_S(P) = 1.8 \text{ K}$  ( $P = 1.64 \text{ kPa}$ ),  $(dT/dP)_S = 1.79 \times 10^{-4} \text{ K/Pa}$ ,  $K = 10.4 \text{ W}\cdot\text{cm}^{-5/3}\cdot\text{K}^{-1/3}$ ,  $h = 20 \text{ cm}$ ,  $Q = 25 \text{ mW}\cdot\text{cm}^{-3}$ . We then find from Eq. (3.42) that  $f > 0.351$ , and using the empirical fit quoted above we find further that  $\rho < 0.75$ . This pitch-to-diameter ratio corresponds to a fairly compact tube bank. If we want a thermal power transfer of  $Q = 50 \text{ mW}\cdot\text{cm}^{-3}$ , then  $f > 0.702$  and  $\rho < 0.47$ , corresponding to a somewhat looser lattice. The maximum thermal power transfer allowed by Eq. (3.43) is  $71 \text{ mW}\cdot\text{cm}^{-3}$  ( $f = 1$ ,  $\rho = 0$ ).

**Constant Heat Source in an Irregular Volume.** The problem dealt with in Eq. (3.40) brings to mind the generalization  $\nabla \cdot (\nabla T)^{1/3} + 1 = 0$  in some volume  $V$  and  $T = 0$  on the surface  $S$  of  $V$ . This problem abstracts the mathematical essence of the temperature rise caused by a steady thermal power source in a volume  $V$  well-cooled at its surface  $S$ . I cannot think of a weighty practical application of this problem, but it does help to demonstrate the limitations of variational principles.

The *upper* complementary variational principle is

$$A_+ = \int_V \left( \frac{3}{4} |\nabla T|^{4/3} - T \right) dV, \quad (3.44)$$

where  $T$  is a trial function that obeys the boundary condition  $T = 0$  on the surface  $S$  of  $V$ . This assertion is easily proved by the techniques used in the introduction to this chapter. When  $T = T_*$ , the exact solution to the problem, then  $A_+ = A_*$ , its minimum value, which the following short computation identifies as being proportional to the *average* temperature rise in the volume  $V$ :

$$A_* = \int_V \left( \frac{3}{4} |\nabla T_*|^{4/3} - T_* \right) dV \quad (3.45a)$$

$$= \int_V \left( \frac{3}{4} \nabla \cdot [T_* \cdot (\nabla T_*)^{1/3}] - \frac{1}{4} T_* \right) dV \quad (3.45b)$$

$$= \frac{3}{4} \int_S T_* (\nabla T_*)^{1/3} \cdot d\vec{S} - \frac{1}{4} \int_V T_* dV = -\frac{1}{4} \int_V T_* dV \quad (3.45c)$$

since  $T_*(S) = 0$ .

The average temperature rise is less useful than the maximum temperature rise, so the variational method now offers us much less than in the earlier case of the irregular duct. This short discussion has been included here to warn the reader that, while the method of complementary variational principles is powerful, it is no panacea.

## CHAPTER 4

## MAXIMUM AND MINIMUM PRINCIPLES

**Introduction.** In the discussion of Okamura's experiments in Chap. 2, we used similarity solutions as the basis for an approximate treatment of the problem, showing thereby at least one way to extend the applicability of similarity solutions. Another way is to compare them with other solutions. Here we use the word "compare" in the strict sense of Hardy, Littlewood, and Polya<sup>15</sup>: two functions are comparable in a domain if there is an inequality between them valid for all arguments in the domain. One way to compare functions is by use of maximum and minimum principles. The rather odd terminology "maximum or minimum principles" means this: a function is said to have a maximum (minimum) principle in a domain  $D$  if it achieves its largest (smallest) value on the boundary of  $D$ . Not only does the existence of a maximum or minimum principle allow solutions to be compared with each other, but it is also possible to compare solutions with trial functions which do not satisfy the differential equation. All this is clearer in application than in description, so let us move straightaway to a discussion of the maximum (minimum) principles of the superfluid diffusion equation.

**The Maximum and Minimum Principles.** The steady-state version of Eq. (1.2),

$$\nabla \cdot [K(\nabla T)^{1/3}] = 0, \quad (4.1)$$

has a maximum principle as explained in the following essentially verbatim excerpt from one of my earlier reports<sup>18</sup>:

Equation (4.1) has a maximum principle, i.e., the largest and smallest temperatures lie on the boundary  $B$  of any region  $R$ . To see this, suppose that  $T$  has a relative maximum at some point  $P$  in the interior of  $R$ . In the neighborhood of  $P$ , the level surfaces of  $T$  are closed surfaces enclosing  $P$ . The vector  $-\nabla T$  is the outward normal to these surfaces. Now  $\nabla T = -q^2 \vec{q}/K^3$ , so  $\vec{q} \cdot (-\nabla T) = q^4/K^3 > 0$ , which means that the vector  $\vec{q}$  makes an acute angle with  $-\nabla T$ , the outward normal to the level surfaces of  $T$ . Hence  $\int \int \vec{q} \cdot \vec{ds} > 0$  when taken over a level surface of  $T$ . But since  $\nabla \cdot \vec{q} = 0$  everywhere, this integral must vanish. This is a contradiction, so our original supposition that  $T$  had a relative maximum must be false. A similar argument applies to relative minima.

In the case of a linear equation, the difference of two solutions, being a solution itself, has a maximum and a minimum principle. However, this simple argument does not suffice for Eq. (4.1) because it is nonlinear. Nevertheless, even though the difference of two solutions is *not* necessarily a solution, the difference obeys a maximum and a minimum principle. Suppose the two solutions are  $T_1$  and  $T_2$ . Then

$$\begin{aligned}
 -K^3 \nabla(T_1 - T_2) \cdot (\vec{q}_1 - \vec{q}_2) &= (q_1^2 \vec{q}_1 - q_2^2 \vec{q}_2) \cdot (\vec{q}_1 - \vec{q}_2) \\
 &= q_1^4 - (q_1^2 + q_2^2) \vec{q}_1 \cdot \vec{q}_2 + q_2^4 \\
 &> q_1^4 - (q_1^2 + q_2^2) q_1 q_2 + q_2^4 \\
 &= (q_1^3 - q_2^3)(q_1 - q_2) \\
 &= (q_1^2 + q_1 q_2 + q_2^2)(q_1 - q_2)^2 > 0. \quad (4.2)
 \end{aligned}$$

Thus  $\vec{q}_1 - \vec{q}_2$  makes an acute angle with the normal  $-\nabla(T_1 - T_2)$  to the level surfaces of  $T_1 - T_2$ . Since  $\nabla \cdot (\vec{q}_1 - \vec{q}_2) = 0$ , these level surfaces cannot be closed, i.e.,  $T_1 - T_2$  cannot have either a relative maximum or a relative minimum in the interior of any region  $R$ .

This argument can be extended to functions  $T_1$  obeying differential and boundary inequalities. Suppose, for example, we have a function  $T_1$  for which  $\nabla \cdot [K(\nabla T_1)^{1/3}] > 0$  and for which  $T_1(B) < T_2(B)$ , where  $T_2$  is a solution of Eq. (4.1). Then  $\nabla \cdot \vec{q}_1 < 0$  and so  $\nabla \cdot (\vec{q}_1 - \vec{q}_2) < 0$ . Thus  $T_1 - T_2$  cannot have a relative maximum in  $B$ . For then,  $\int \int (\vec{q}_1 - \vec{q}_2) \cdot d\vec{S}$  must be  $> 0$  when taken over a closed level surface around the maximum. This contradicts  $\nabla \cdot (\vec{q}_1 - \vec{q}_2) < 0$ . Therefore, the largest value of  $T_1 - T_2$  lies on  $B$ . Then  $T_1 - T_2 < (T_1 - T_2)_{\max} < 0$  since  $T_1(B) < T_2(B)$ , and thus  $T_1 < T_2$  everywhere in  $R$ . The same argument applies when the inequalities are reversed and the words "largest" and "maximum" are replaced by the words "smallest" and "minimum," respectively.

**Constant Heat Source in a Square of Side 2.** Let us return to the problem of a constant heat source in an irregular volume dealt with at the end of Chap. 3. For definiteness let us choose the volume to be a very long square prism—thus a square of side 2. We wish to find information about the solution  $T$  of the (two-dimensional) equation  $\nabla \cdot (\nabla T)^{1/3} + 1 = 0$  for which  $T = 0$  on the perimeter  $P$  of the square  $S$  whose vertices are  $(\pm 1, \pm 1)$ .

We can make a quick start by noting that the function  $T_1 = (R^4 - r^4)/32$  is a solution of our equation in cylindrical coordinates. Here  $R^4$  is a constant of integration yet to be chosen. The difference  $T_1 - T$  has its maximum and minimum on  $P$ . Since  $T(P) = 0$ ,

$$\min[T_1(P)] < T_1 - T < \max[T_1(P)] . \quad (4.3)$$

Owing to the geometric symmetry of the problem, we need only consider the values of  $T_1(P)$  on the interval  $x = 1, 0 \leq y \leq 1$ , where  $T_1(P) = [R^4 - (1 + y^2)^2]/32$ . Thus  $\min[T_1(P)] = (R^4 - 4)/32$  and  $\max[T_1(P)] = (R^4 - 1)/32$ . Now since  $T_1(0, 0) = R^4/32$ , it follows from Eq. (4.3) that  $1/32 \leq T(0, 0) \leq 1/8$ .

This is not a very satisfactory result because the bounds on  $T(0, 0)$  differ from one another by a factor of four. We can improve our estimate of  $T(0, 0)$  at the cost of some additional computational labor in the following way. Suppose we find a vector  $\vec{q}_1$ , such that  $\nabla \cdot \vec{q}_1 = 1$  in  $S$ , and define  $T_1$  as any solution of  $\nabla T_1 = -q_1^2 \vec{q}_1$ . Let  $T_2$  be the exact solution of our problem. Then the proof embodied in Eq. (4.2) shows that  $T_1 - T_2$  has a minimum and a maximum principle in the square  $S$ .

Suppose we try  $\vec{q}_1 = \frac{1}{2}\vec{r} + \nabla\phi$ , where  $\nabla^2\phi = 0$  in  $S$ . Then  $\nabla \cdot \vec{q}_1 = 1$  as required. We choose for this problem  $\phi = a(x^4 - 6x^2y^2 + y^4)$ , where  $a$  is a constant yet to be determined. The function  $\phi$  has the three symmetries of the square:  $x \rightarrow -x$ ,  $y \rightarrow -y$ , and  $x \rightarrow y \rightarrow x$ . Our computational problem is to choose  $a$  to minimize the difference of the extreme values of  $T_1$  on  $P$ , the perimeter of  $S$ . Again owing to the geometric symmetry of the problem we need only consider the segment  $x = 1, 0 \leq y \leq 1$ . A straightforward but somewhat tedious calculation shows that

$$\begin{aligned} T_1(1, 0) - T_1(1, y) &= \frac{32}{5}a^3y^{10} + 3a^2y^8 - \frac{1}{6}(384a^3 + 120a^2 - 3a)y^6 \\ &\quad - \frac{1}{4}\left(512a^3 - 328a^2 + 14a - \frac{1}{8}\right)y^4 - \frac{1}{2}\left(192a^3 + 40a^2 + a - \frac{1}{8}\right)y^2 . \end{aligned} \quad (4.4)$$

A simple numerical computation shows that the value  $a = 0.0464894$  minimizes the difference of extrema at the value  $\epsilon = 1.78425 \times 10^{-3}$ ; the minimum of  $T_1(1, y)$  is  $T_1(1, 0)$  and the maximum is  $T_1(1, 0) + \epsilon$ . Then

$$0 < -T_2(x, y) + T_1(x, y) - T_1(1, 0) < \epsilon . \quad (4.5)$$

Another short computation integrating  $(T_1)_x = -q_1^2 q_1 \vec{x}$  along the line  $y = 0$  from  $x = 0$  to  $x = 1$  gives

$$T_1(0, 0) - T_1(1, 0) = 6.162154 \times 10^{-2} \equiv M . \quad (4.6)$$

From Eqs. (4.5) and (4.6) it then follows that

$$\frac{\epsilon}{2} > T_2(0, 0) - \left(M - \frac{\epsilon}{2}\right) > -\frac{\epsilon}{2} , \quad (4.7a)$$

or

$$8.92125 \times 10^{-4} > T_2(0, 0) - 6.07294 \times 10^{-2} > -8.92125 \times 10^{-4} , \quad (4.7b)$$

or finally

$$T_2(0, 0) = 6.07294 \times 10^{-2} \pm 1.47\% , \quad (4.7c)$$

which is a rather acceptable result. This result can be extended to squares whose sides have other lengths by noting that the partial differential equation is invariant to the group  $T' = \lambda^4 T$ ,  $x' = \lambda x$ ,  $y' = \lambda y$ , so that  $T(0, 0)$  varies as the fourth power of the side of the square.

**Pulsed-Source Problem in Spherical Geometry.** Another problem in which maximum and minimum principles play an essential role is the pulsed-source problem in spherical geometry. The reader may recall that in plane geometry the pulsed-source problem has the similarity solution (1.31) and (1.32) for the temperature rise  $T$ . In spherical geometry, Eq. (1.3) takes the form

$$\frac{\partial T}{\partial t} = \frac{1}{r^2} \frac{\partial}{\partial r} \left[ r^2 \left( \frac{\partial T}{\partial r} \right)^{1/3} \right] . \quad (4.8)$$

The boundary and initial conditions corresponding to the pulsed-source problem are

$$T(r, 0) = 0 \quad (r > 0) , \quad (4.9a)$$

$$T(\infty, t) = 0 , \quad (4.9b)$$

$$\int_0^\infty 4\pi r^2 T \, dr = Q \quad (t > 0) . \quad (4.9c)$$

The partial differential equation (4.8) is invariant to the family of groups (1.5) subject to the subsidiary relation (1.6) with  $M = 2$ ,  $N = -3$ , and  $L = -4$ . The boundary condition (4.9c) requires that  $\alpha = -3$ , so that  $\beta = -2/3$ . With these values, the similarity solution (1.7) becomes  $T = t^{9/2} y(rt^{3/2})$ .

This last form is unsatisfactory because it represents a temperature distribution that peaks up as time goes on rather than one which spreads out. This defect is fundamental and means that the pulsed-source problem in spherical geometry has no solution of the form (1.7). It does, however, have solutions of a very closely related form, as we shall see next.

In addition to its invariance to the groups (1.5), Eq. (4.8) is invariant to the group of translations in time:  $T' = T$ ,  $t' = t + \lambda$ ,  $r' = r$ . Solutions invariant to this group must be functions of the time difference  $t - t_0$ , where  $t_0$  is some fiducial time that is determined by the boundary and initial conditions. These considerations suggest that we look for similarity solutions of the form

$$T = (t_0 - t)^{9/2} y [r(t_0 - t)^{3/2}] . \quad (4.10)$$

If we substitute this form into Eq. (4.8), we obtain for  $y$  the following ordinary differential equation:

$$\frac{1}{\xi^2} \frac{d}{d\xi} (\xi^2 \dot{y}^{1/3}) + \frac{3}{2} \xi \dot{y} + \frac{9}{2} y = 0 \quad , \quad \xi = r(t_0 - t)^{3/2} . \quad (4.11)$$

After multiplication by  $\xi^2$ , this can be integrated once to give

$$\xi^2 \dot{y}^{1/3} + \frac{3}{2} \xi^3 y = C \quad , \quad (4.12)$$

where  $C$  is a constant of integration. If  $y$  is regular at the origin  $\xi = 0$ , then  $C = 0$ , in which case Eq. (4.12) can be integrated a second time to give

$$y = \left( a + \frac{27}{16} \xi^4 \right)^{-1/2} \quad , \quad (4.13)$$

where  $a$  is a second constant of integration.

The solution (4.13) is an exact solution of the superfluid diffusion equation. Its overall form  $c = (t_0 - t)^{9/2} y [r(t_0 - t)^{3/2}]$  was chosen so that the total heat  $Q = 4\pi \int_0^\infty r^2 c \, dr$  would be conserved. But with the form (4.13) for  $y$ , the  $Q$ -integral diverges. Thus the solution (4.13) cannot fulfill the initial condition of a finite source pulse, and so, strictly speaking, the solution to the pulsed-source problem is not a similarity solution of the form (4.10).

Suppose we consider a pulsed source in which the finite heat deposition is such that the initial temperature distribution is given by the similarity solution (4.13) out to a radius  $r = R$ , but is zero for  $r > R$ . If  $R$  is large enough, the initial effect of the region  $r > R$  on the temperature distribution near  $r = 0$  should be small. So the

central temperature should begin falling like  $(t_0 - t)^{9/2}$ . Since the region  $r > R$  is initially colder than in the similarity solution (4.13), it seems plausible for the central temperature to continue falling faster than  $(t_0 - t)^{9/2}$ . Indeed, we might expect that any temperature distribution that is initially smaller than some similarity solution of the family (4.13) will always remain smaller. Thus the central temperature should be bounded from above by  $a^{-1/2}(t_0 - t)^{9/2}$ , which means it should vanish at some finite time after the pulse! The proof of these last assertions, given next, involves some complicated but rather standard analysis involving maximum and minimum principles.

**Proof of the Foregoing Assertions.** Let us consider the infinitesimal difference  $\delta c$  between two neighboring solutions of the superfluid diffusion equation  $c_t = r^{-2}(r^2 c_r^{1/3})_r$ . It obeys the *linear* partial differential equation  $(\delta c)_t = r^{-2}[r^2(c_r^{-2/3}/3)(\delta c)_r]_r$ , which has the form

$$\frac{1}{r^2} \frac{\partial}{\partial r} \left( r^2 k \frac{\partial \phi}{\partial r} \right) = \frac{\partial \phi}{\partial t}, \quad k > 0. \quad (4.14)$$

Equation (4.14) describes heat conduction in spherical geometry with a thermal conductivity  $k$ . The boundary and initial conditions that interest us are

$$\phi(r, 0) > 0, \quad (4.15a)$$

$$\phi(\infty, t) = 0, \quad (4.15b)$$

$$\phi \text{ regular at } r = 0. \quad (4.15c)$$

What we should like to show is that  $\phi(r, t) > 0$  for all  $t > 0$ . In that case, two solutions  $c_1$  and  $c_2$  of the superfluid diffusion equation that obey the boundary conditions (4.15b) and (4.15c) and the initial condition  $c_1 > c_2$  are always ordered so that  $c_1 > c_2$ .

We begin first by considering a function  $\psi$  that obeys the strict differential inequality

$$\frac{1}{r^2} \frac{\partial}{\partial r} \left( r^2 k \frac{\partial \psi}{\partial r} \right) - \frac{\partial \psi}{\partial t} < 0 \quad (4.16)$$

and the boundary condition (4.15c) in the rectangle  $\Sigma$  in the  $(r, t)$ -plane (see Fig. 4.1). The minimum value of  $\psi$  cannot lie in the interior of  $\Sigma$ , for if it did, say at a point  $P$ , then  $\psi_t(P) = 0$ ,  $\psi_r(P) = 0$ , and  $\psi_{rr}(P) \geq 0$ . These conditions contradict the strict inequality (4.16). Moreover, the minimum value of  $\psi$  cannot lie at an interior point  $Q$  of  $S_4$ , for if it did, then  $\psi_r(Q) = 0$  and  $\psi_{rr}(Q) \geq 0$ . Then

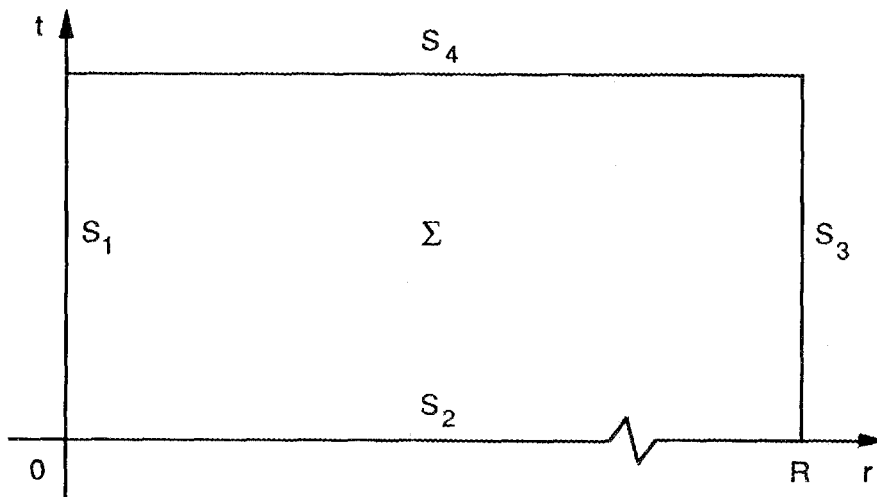


Fig. 4.1. The rectangle in the  $(r, t)$  plane used in proving the minimum principle for the differential inequality (4.16).

from Eq. (4.16) it follows that  $\psi_t(Q) > 0$ , which means that there must be yet smaller values of  $\psi$  in the neighborhood of  $Q$  inside  $\Sigma$ , contrary to hypothesis.

Finally, the minimum value of  $\psi$  cannot lie at an interior point of  $S_1$ , but in order to prove this, we shall have to consider in detail the consequences of boundary condition (4.15c). First of all, any solution  $c$  of the superfluid diffusion equation (4.8) that is regular at the origin must behave near  $r = 0$  like  $a + br^4 + \dots$ , for only then can the right-hand side of Eq. (4.8) have a finite, nonzero limit as  $r \rightarrow 0$ . In that case  $c_r^{-2/3} \sim r^{-2}$  near  $r = 0$  and thus so does  $k$  in Eq. (4.14). Furthermore,  $\psi$ , being the infinitesimal difference between two solutions of the superfluid diffusion equation, also has the form  $a + br^4 + \dots$  near  $r = 0$ . If we substitute this form for the first term on the left-hand side of Eq. (4.16) we find that it equals  $12b \cdot \lim_{r \rightarrow 0} (r^2 k)$  at  $r = 0$ . If the minimum of  $\psi$  occurs at an interior point  $T$  of  $S_1$ , then  $\psi_t(T) = 0$ . Therefore  $b(T) < 0$ , which means that there are yet smaller values of  $\psi$  in the neighborhood of  $T$  inside  $\Sigma$ , a contradiction. The minimum of  $\psi$  must therefore lie on  $S_2$  or  $S_3$ .

When  $\phi$  satisfies the equality (4.14), we introduce the auxiliary function

$$\psi = \phi + \epsilon t \quad , \quad \epsilon > 0 \quad , \quad (4.17)$$

which satisfies the differential inequality (4.16). Furthermore,  $\psi$  behaves like  $a + br^4 + \dots$  near  $r = 0$ , as it should. Therefore, its minimum value in  $\Sigma$  must lie on  $S_2$

or  $S_3$ ; call it  $m_\psi$  and let it be attained at point  $P$ . Let  $m_\phi$  be the smallest value  $\phi$  attains on  $S_2$  and  $S_3$  (not yet proved to be its minimum value in  $\Sigma$ !). Then from Eq. (4.17), for any point  $Q$  in  $\Sigma$ ,

$$\phi(Q) + \epsilon t_Q = \psi(Q) > m_\psi \quad (4.18)$$

and

$$m_\psi = \psi(P) = \phi(P) + \epsilon t_P \geq m_\phi + \epsilon t_P . \quad (4.19)$$

Thus, combining Eqs. (4.18) and (4.19), we find

$$\phi(Q) > m_\phi + \epsilon(t_P - t_Q) . \quad (4.20)$$

Finally, if we let  $\epsilon \rightarrow 0$ , we see that  $\phi$  is always  $\geq$  the smallest value it attains on  $S_2$  and  $S_3$ , so that its minimum must lie on  $S_2$  or  $S_3$ .

If  $\phi \geq 0$  on  $S_2$  and  $\phi = 0$  on  $S_3$ , then its minimum value must be zero. Therefore,  $\phi \geq 0$  everywhere in  $\Sigma$ , as was to be proved. The last step is to let  $R \rightarrow \infty$ .

**Discussion.** Suppose we establish an initial temperature rise  $T_1$  inside a sphere of radius  $R$ . We can use the foregoing results to obtain an upper limit to the time at which the temperature rise disappears. To do so, we need to find a similarity solution whose initial form at  $t = 0$ , namely,  $T = t_0^{9/2}(a + 27r^4t_0^6/16)^{-1/2}$ , exceeds  $T_1$  for  $r \leq R$ . The best (smallest) upper limit  $t_0$  will correspond to an initial form  $T$  that just equals  $T_1$  at  $r = R$  (see Fig. 4.2). The choices of  $a$  and  $t_0$  are therefore constrained by the relation

$$T_1 = t_0^{9/2} (a + 27R^4t_0^6/16)^{-1/2} \quad (4.21)$$

or

$$t_0^9 - \frac{27R^4T_1^2}{16}t_0^6 - aT_1^2 = 0 . \quad (4.22)$$

Equation (4.22) has one real root, which is always larger than

$$t_{0*} = \frac{3}{2} \left( \frac{R^4T_1^2}{2} \right)^{1/3} \quad (4.23)$$

and approaches  $t_{0*}$  as  $a$  becomes smaller (see Fig. 4.3).

The radius  $R$ , the temperature rise  $T_1$ , and the source strength  $Q$  are related by

$$Q = \frac{4\pi}{3}T_1R^3 , \quad (4.24)$$

ORNL-DWG 89M 2628 FED

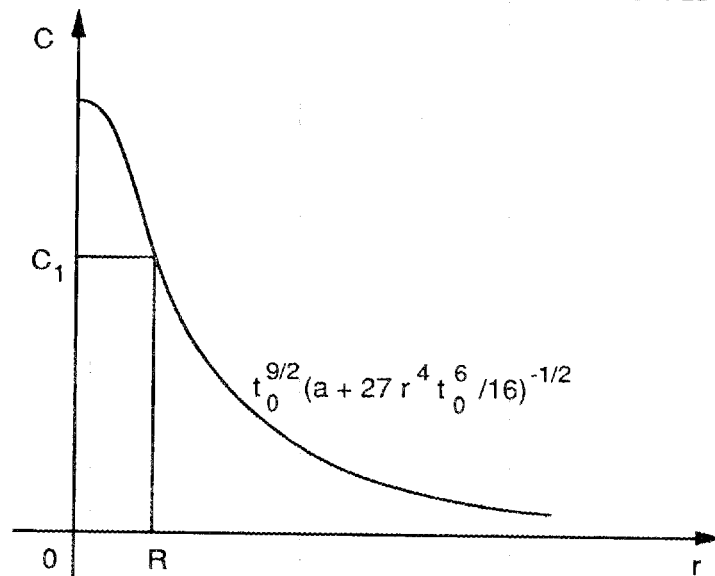


Fig. 4.2. A uniform initial temperature rise in the sphere of radius  $R$  compared with the initial temperature distribution of a similarity solution.

ORNL-DWG 89M-2629 FED

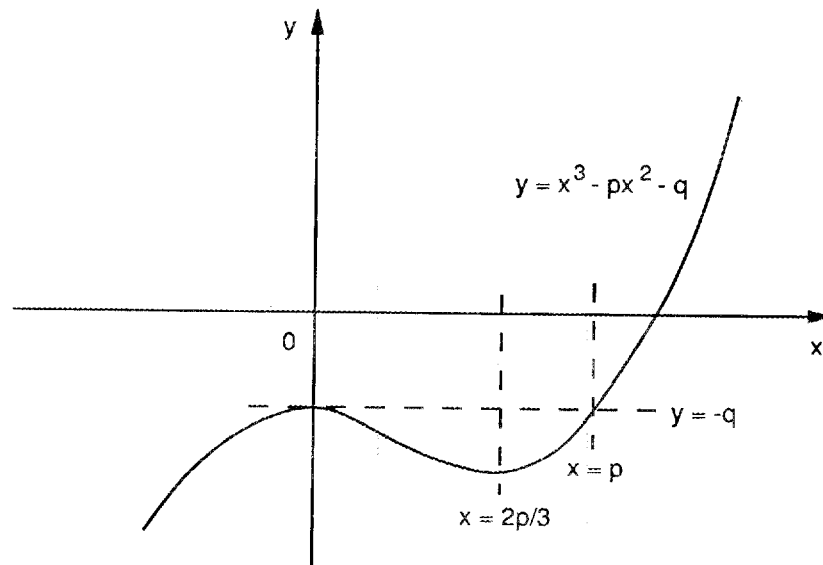


Fig. 4.3. An auxiliary sketch depicting the relation of the real root of Eq. (4.22) to the coefficient  $p$ .

and if we use Eq. (4.24) to eliminate  $R$  in Eq. (4.23), we obtain

$$t_{0*} = \frac{3}{2^{4/3}} \left( \frac{3}{4\pi} \right)^{4/9} \cdot Q^{4/9} T_1^{2/9} . \quad (4.25)$$

The numerical constant in (4.25) equals 0.629889... .

Equation (4.25) is correct in special units in which  $K$  and  $S$  are numerically equal to 1. In ordinary units, Eq. (4.25) must be written

$$t_{0*} = 0.629889 (Q^4 T_1^2 S^5)^{1/9} / K \quad (4.26)$$

When the bath temperature is 1.8 K (and the pressure is 1 atm),  $S = 0.410 \text{ J}\cdot\text{cm}^{-3}\cdot\text{K}^{-1}$  and  $K = 10.4 \text{ W}\cdot\text{cm}^{-5/3}\cdot\text{K}^{-1/3}$ . In the one-dimensional experiment of Lottin and van Sciver,<sup>4</sup> a heat pulse of 0.92 J was deposited at a point in a 6-mm tube. Taking  $T_1 = T_\lambda - T_b = 0.37 \text{ K}$ , we find, from Eq. (4.26),  $t_{0*} = 28.5 \text{ ms}$ . So we expect the temperature rise to be extinguished in less than 30 ms; this is quite different from the 1-D experiment of Lottin and van Sciver in which a 0.050 K temperature rise was still perceptible after one full second. This rather remarkable prediction has not yet been tested experimentally and is a tempting target for further study.

**Pulsed-Source Problem in Cylindrical Geometry.** In cylindrical geometry, Eq. (1.3) takes the form

$$\frac{\partial T}{\partial t} = \frac{1}{r} \frac{\partial}{\partial r} \left[ r \left( \frac{\partial T}{\partial r} \right)^{1/3} \right] . \quad (4.27)$$

We wish to solve it subject to the boundary and initial conditions

$$T(r, 0) = 0 \quad (r > 0) , \quad (4.28a)$$

$$T(\infty, t) = 0 , \quad (4.28b)$$

$$\int_0^\infty 2\pi r T \, dr = Q \quad (t > 0) . \quad (4.28c)$$

Equation (4.27) is invariant to the mixed stretching-translation group

$$T' = \lambda^{-2} T , \quad (4.29a)$$

$$t' = t + \frac{1}{\beta} \ln \lambda \quad (0 < \lambda < \infty) , \quad (4.29b)$$

$$r' = \lambda r , \quad (4.29c)$$

where  $\beta$  is an arbitrary constant not yet determined. The most general form for  $T(r, t)$  invariant to a group of the family (4.29) is

$$T = e^{-2\beta t} y(re^{-\beta t}) , \quad (4.30)$$

where  $y$  is an arbitrary function of the single argument  $\xi = re^{-\beta t}$ . Furthermore, Eq. (4.30) has the right form to satisfy the boundary condition (4.28c):

$$2\pi \int_0^\infty y(\xi) \xi d\xi = Q . \quad (4.31)$$

If we substitute Eq. (4.30) into Eq. (4.27), we get

$$\frac{1}{\xi} \frac{d}{d\xi} (\xi \dot{y}^{1/3}) + \beta (2y + \xi \dot{y}) = 0 , \quad \xi = re^{-\beta t} . \quad (4.32)$$

After multiplication by  $\xi$ , this can be integrated to give

$$\xi \dot{y}^{1/3} + \beta \xi^2 y = C , \quad (4.33)$$

where  $C$  is a constant of integration. If  $y$  is regular at the origin  $\xi = 0$ , then  $C = 0$ . Then Eq. (4.14) can be integrated again to give

$$y = \left( a + \frac{\beta^3}{2} \xi^4 \right)^{-1/2} , \quad (4.34)$$

where  $a$  is another constant of integration.

Again the  $Q$ -integral diverges, so the solution (4.34) cannot fulfill the initial condition of a finite heat pulse. But again, by a repetition of the argument of the last section, we expect it to exceed for all time any solution that it exceeds at  $t = 0$ . Thus the central temperature should be bounded from above by  $a^{-1/2} e^{-2\beta t}$ , which means it should fall exponentially with time.

As before, the choices of  $a$  and  $\beta$  in Eq. (4.34) are constrained by the initial condition

$$T_1 = \left( a + \frac{\beta^3}{2} R^4 \right)^{-1/2} , \quad (4.35)$$

from which it follows that the largest possible value of  $\beta$  is

$$\beta_* = \left( \frac{2}{R^4 T_1^2} \right)^{1/3} . \quad (4.36)$$

If we now define  $t_{0*} = 1/2\beta_*$ , the relaxation time of the central temperature, we find

$$t_{0*} = \left( \frac{R^4 T_1^2}{16} \right)^{1/3} . \quad (4.37)$$

The source strength  $Q$  is related to  $R$  and  $T_1$  by

$$Q = \pi R^2 T_1 , \quad (4.38)$$

so that

$$t_{0*} = \left( \frac{Q^2}{16\pi^2} \right)^{1/3} . \quad (4.39)$$

Whereas in the spherical case  $Q$  has the dimensions of J, in the cylindrical case it has the dimensions of J·m<sup>-1</sup>. So in ordinary units,

$$t_{0*} = \frac{1}{K} \left( \frac{Q^2 S}{16\pi^2} \right)^{1/3} . \quad (4.40)$$

An energy deposition  $Q$  of 1 J·cm<sup>-1</sup> results in a relaxation time of 13.2 ms.

## CONCLUDING REMARKS

The material in the preceding chapters constitutes the bulk of the knowledge about the superfluid diffusion equation won during the four-year collaboration between Oak Ridge National Laboratory and the University of Wisconsin-Madison. Actually, somewhat more was done: at Prof. van Sciver's suggestion (1) I developed a method of design of tube-in-shell heat exchangers,<sup>19</sup> which has since been employed,<sup>20</sup> and (2) I calculated the temperature distribution in transfer lines intended for in-orbit transfer of He-II.<sup>21</sup> Both of these studies have been omitted here because they are based on the one-dimensional, steady superfluid diffusion equation and thus do not deal with the partial differential aspect of this equation. A further study that does deal with this partial differential aspect is one I made of thermal boundary layer development in rapidly flowing He-II, but as the results were neither elegant nor especially interesting, I have decided to omit this study, too.

When analytic methods are exhausted, the conventional recourse is to numerical methods. Even here, the subtleties of the superfluid diffusion equation make themselves felt. The simplest finite-difference representation of Eq. (1.4) is the explicit marching scheme

$$T_{n,m+1} = T_{n,m} + \frac{k}{h^{4/3}} \left[ (T_{n+1,m} - T_{n,m})^{1/3} - (T_{n,m} - T_{n-1,m})^{1/3} \right], \quad (\text{C.1})$$

where  $T_{n,m}$  is an abbreviation for  $T(z = nh, t = mk)$ . Now as it happens, this scheme is always unstable, but in a rather special way. Unstable integration schemes are often beset by the growth of wild oscillations, so let us test Eq. (C.1) to see if it admits solutions of the form

$$T_{n,m} = (-)^n e_m. \quad (\text{C.2})$$

Substituting Eq. (C.2) into Eq. (C.1), we find

$$e_{m+1} = e_m - \frac{2^{4/3}k}{h^{4/3}} e_m^{1/3}. \quad (\text{C.3})$$

Equation (C.3) has as a solution the two-cycle

$$e_m = \pm (-)^m \frac{\sqrt{2}k^{3/2}}{h^2} \quad (\text{C.4})$$

for all values of  $k/h^{4/3}$ . From this we might expect the solutions of Eq. (C.1) to be perturbed by high-frequency fluctuations of constant amplitude given by Eq. (C.4).

To test this conclusion, I performed calculations of the pulsed-source problem in plane geometry (for which the solution is known) and found it to be so.<sup>18</sup> Others have been beset by this problem, too.<sup>22</sup> The brute-force cure is to take the time step short enough that the amplitude of the unwanted fluctuations has little impact on the differences on the right-hand side of Eq. (C.1). This often condemns us to using a very short time step and thus to consuming much computing time.

The instabilities of the explicit scheme can be avoided by going to an implicit scheme, such as

$$\frac{T_{n+1,m+1} - 2T_{n,m+1} + T_{n-1,m+1}}{h^2} = 3q_{n,m}^2 \frac{T_{n,m+1} - T_{n,m}}{k}, \quad (\text{C.5a})$$

$$q_{n,m} = \left( \frac{T_{n+1,m} - T_{n-1,m}}{2h} \right)^{1/3}, \quad (\text{C.5b})$$

for which no such oscillating solution as Eq. (C.4) is possible. Numerical experiments confirm the stability of this scheme. I have not delved further into this matter, but for those intending to develop numerical programs, the foregoing considerations need to be borne in mind.

Shakespeare tells us that “an honest tale speeds best being plainly told,” so, having exhausted my thoughts on the superfluid diffusion equation, I now bring this report bluntly to a close.

## REFERENCES

1. L. Dresner, *Similarity Solutions of Nonlinear Partial Differential Equations*, Pitman Publishing, Inc., Marshfield, Mass., 1983.
2. R. E. Pattle, "Diffusion from an Instantaneous Point Source with a Concentration-Dependent Coefficient," *Q. J. Mech. Appl. Math.* **XII**, Pt. 4, 407-9 (1959).
3. S. W. van Sciver, "Transient Heat Transport in He-II," *Cryogenics* **19**, 385 (1979).
4. J. C. Lottin and S. W. van Sciver, "Heat Transport Mechanisms in a 2.3-meter-long Cooling Loop Containing He-II," p. 269 in *Proceedings of the Ninth International Cryogenic Engineering Conference, Kobe, Japan, May 11-14, 1982*, Butterworths, Guildford, Surrey, U.K., 1982.
5. P. Seyfert, J. Lafferanderie, and G. Claudet, "Time-Dependent Heat Transport in Subcooled Superfluid Helium," *Cryogenics* **22**, 401 (1982).
6. T. Okamura, Y. Yoshizawa, A. Sato, K. Ishito, S. Kabashima, and S. Shioda, "Time-Dependent Heat Transport in Pressurized Superfluid Helium," *Cryogenics* **29**, 1070 (1989).
7. L. Dresner, "A Rapid, Semiempirical Method of Calculating the Stability Margins of Superconductors Cooled with Subcooled He-II," *IEEE Trans. Magn.* **MAG-23** (2), 918-21 (1987); "Stability Margins of Superconductors Cooled with Subcooled He-II," *Cryogenics* **29**, 668-73 (1989).
8. J. Pfothenauer and S. W. van Sciver, "Stability Measurements of a Superconductor Cooled by a Two-Dimensional Channel of He-II," *Adv. Cryog. Eng.* **31**, 391-8 (1986).
9. L. Dresner, "Bubble Growth in Superheated He-II," *Cryogenics* **29**, 509-12 (1989).
10. J. Wilks, *The Properties of Liquid and Solid Helium*, Clarendon Press, Oxford, 1967.
11. L. Dresner, "Transient Heat Transfer in Superfluid Helium," *Adv. Cryog. Eng.* **27**, 411-9 (1982).
12. S. W. van Sciver, *Helium Cryogenics*, Plenum Press, New York, 1986.
13. B. Noble and M. J. Sewell, "On Dual Extremum Principles in Applied Mathematics," *J. Inst. Math. Its Appl.* **9**, 123-93 (1972).
14. A. M. Arthurs, *Complementary Variational Principles*, Clarendon Press, Oxford, 1970.

15. G. H. Hardy, J. E. Littlewood, and G. Polya, *Inequalities*, 2nd ed., Cambridge Univ. Press, Cambridge, 1952.
16. G. Polya and S. Szegő, *Isoperimetric Inequalities in Mathematical Physics*, Princeton Univ. Press, Princeton, N.J., 1951.
17. L. Dresner, "Gorter-Mellink Heat Transport in He-II Transverse to Tube Banks and Through Ducts of Nonuniform Cross Section," pp. 256-60 in *Proceedings of the Twelfth International Cryogenic Engineering Conference (ICEC12), Southampton, England, July 12-15, 1988*, ed. by R. J. Scurlock and C. O. Bailey, Butterworths, Guildford, Surrey, U.K., 1988.
18. L. Dresner, *Nonlinear Differential Equations*, ORNL/TM-10655, Martin Marietta Energy Systems, Inc., Oak Ridge Natl. Lab., January 1988.
19. L. Dresner, "Design of Tube-in-Shell Heat Exchangers for He-II, *AIChE Symp. Ser.* **82** (251), 81-85 (1986).
20. J. G. Weisend II, Y. Huang, and S. W. van Sciver, "Testing of Two Heat Exchangers in He-II," presented at the Seventh Intersociety Cryogenic Symposium, Houston, Texas, January 1989.
21. L. Dresner, A. Kashani, and S. W. van Sciver, "Studies of Heat Transport to Forced Flow He-II," *Cryogenics* **26**, 111-4 (1986).
22. A. Kashani, "Forced Convection heat Transfer in He-II," Ph.D. thesis, University of Wisconsin, Madison, 1986.

**INTERNAL DISTRIBUTION**

1. D. B. Batchelor
2. J. B. Drake
- 3-17. L. Dresner
18. M. S. Lubell
19. C. W. Nestor, Jr.
20. M. W. Rosenthal
21. J. Sheffield
22. G. V. Wilson
- 23-24. Laboratory Records Department
25. Laboratory Records, ORNL-RC
26. Document Reference Section
27. Central Research Library
28. Fusion Energy Division Library
- 29-30. Engineering Technology/Fusion Energy Division Publications Office
31. ORNL Patent Office

**EXTERNAL DISTRIBUTION**

32. Office of the Assistant Manager for Energy Research and Development, U.S. Department of Energy, Oak Ridge Operations Office, Oak Ridge, TN 37831
33. J. D. Callen, Department of Nuclear Engineering, University of Wisconsin, Madison, WI 53706-1687
34. R. W. Conn, Department of Chemical, Nuclear, and Thermal Engineering, University of California, Los Angeles, CA 90024
35. N. A. Davies, Acting Director, Office of Fusion Energy, Office of Energy Research, ER-50 Germantown, U.S. Department of Energy, Washington, DC 20545
36. S. O. Dean, Fusion Power Associates, Inc., 2 Professional Drive, Suite 248, Gaithersburg, MD 20879
37. H. K. Forsen, Bechtel Group, Inc., Research Engineering, P. O. Box 3965, San Francisco, CA 94105
38. J. R. Gilleland, L-644, Lawrence Livermore National Laboratory, P.O. Box 5511, Livermore, CA 94550
39. R. W. Gould, Department of Applied Physics, California Institute of Technology, Pasadena, CA 91125
40. R. A. Gross, Plasma Research Laboratory, Columbia University, New York, NY 10027

41. D. M. Meade, Princeton Plasma Physics Laboratory, P.O. Box 451, Princeton, NJ 08543
42. M. Roberts, International Programs, Office of Fusion Energy, Office of Energy Research, ER-52 Germantown, U.S. Department of Energy, Washington, DC 20545
43. W. M. Stacey, School of Nuclear Engineering and Health Physics, Georgia Institute of Technology, Atlanta, GA 30332
44. D. Steiner, Nuclear Engineering Department, NES Building, Tibbetts Avenue, Rensselaer Polytechnic Institute, Troy, NY 12181
45. R. Varma, Physical Research Laboratory, Navrangpura, Ahmedabad 380009, India
46. Bibliothek, Max-Planck Institut für Plasmaphysik, Boltzmannstrasse 2, D-8046 Garching, Federal Republic of Germany
47. Bibliothek, Institut für Plasmaphysik, KFA Jülich GmbH, Postfach 1913, D-5170 Jülich, Federal Republic of Germany
48. Bibliothek, KfK Karlsruhe GmbH, Postfach 3640, D-7548 Karlsruhe 1, Federal Republic of Germany
49. Bibliothèque, Centre de Recherches en Physique des Plasmas, Ecole Polytechnique Fédérale de Lausanne, 21 Avenue des Bains, CH-1007 Lausanne, Switzerland
50. R. Aymar, CEN/Cadarache, Département de Recherches sur la Fusion Contrôlée, F-13108 Saint-Paul-lez-Durance Cedex, France
51. Bibliothèque, CEN/Cadarache, F-13108 Saint-Paul-lez-Durance Cedex, France
52. Documentation S.I.G.N., Département de la Physique du Plasma et de la Fusion Contrôlée, Association EURATOM-CEA, Centre d'Etudes Nucléaires, B.P. 85, Centre du Tri, F-38041 Grenoble, France
53. Library, Culham Laboratory, UKAEA, Abingdon, Oxfordshire, OX14 3DB, England
54. Library, JET Joint Undertaking, Abingdon, Oxfordshire OX14 3EA, England
55. Library, FOM-Instituut voor Plasmafysica, Rijnhuizen, Edisonbaan 14, 3439 MN Nieuwegein, The Netherlands
56. Library, National Institute for Fusion Science, Chikusa-ku, Nagoya 464-01, Japan
57. Library, International Centre for Theoretical Physics, P.O. Box 586, I-34100 Trieste, Italy
58. Library, Centro Ricerca Energia Frascati, C.P. 65, I-00044 Frascati (Roma), Italy
59. Library, Plasma Physics Laboratory, Kyoto University, Gokasho, Uji, Kyoto, Japan
60. Plasma Research Laboratory, Australian National University, P.O. Box 4, Canberra, A.C.T. 2601, Australia

- 61. Library, Japan Atomic Energy Research Institute, Naka Fusion Research Establishment, 801-1 Mukoyama, Naka-machi, Naka-gun, Ibaraki-ken, Japan
- 62. Library, Japan Atomic Energy Research Institute, Naka Research Establishment, Naka-machi, Naka-gun, Ibaraki-ken, Japan
- 63. P. Komarek, KfK Karlsruhe GmbH, Postfach 3640, D-7548 Karlsruhe 1, Federal Republic of Germany
- 64. S. Shimamoto, Japan Atomic Energy Research Establishment, Tokai Research Establishment, Tokai, Naka-gun, Ibaraki-ken 311-02, Japan

Department of Mathematics, The University of Tennessee,  
Knoxville, TN 37916

- 65. V. Alexiades
- 66. J. S. Bradley
- 67. S. Lenhart

Department of Nuclear Engineering and Engineering Physics,  
University of Wisconsin, Madison, WI 5370

- 68. M. M. Abdelsalam
- 69. R. Boom
- 70. M. Carbon
- 71. M. L. Corradini
- 72. Y. M. Eyssa
- 73. G. L. Kulcinski
- 74. D. C. Larbalestier
- 75. G. A. Moses
- 76. I. N. Sviatoslavsky
- 77. S. W. van Sciver

Swiss Institute for Nuclear Research, CH-5234 Villigen, Switzerland

- 78. G. Vécsey
- 79. J. A. Zichy

80-120. Given distribution as shown in DOE/OSTI-4500, Magnetic Fusion Energy (Dist. Category UC-420)